DOT/FAA/AR-99/8, I

Office of Aviation Research
Washington, D.C. 20591

Improved Barriers to Turbine Engine Fragments: Interim Report I

June 1999

Interim Report

U.S. Department of Transportation
Federal Aviation Administration

NOTICE

This report is available at the Federal Aviation Administration William J. Hughes Technical Center's Full-Text Technical Reports page: www.tc.faa.gov/its/act141/reportpage.html in Adobe Acrobat portable document form (PDF).

Technical Report Documentation Page

1. Report No.	2. Government Accession No.	3. Recipient's Catalog No.
DOT/FAA/AR-99/8, I		

4. Title and Subtitle	5. Report Date
IMPROVED BARRIERS TO TURBINE ENGINE FRAGMENTS: INTERIM REPORT I	June 1999
	6. Performing Organization Code

7. Author(s)	8. Performing Organization Report No.
D.A. Shockey, Jeffrey W. Simons, and David C. Elrich	

9. Performing Organization Name and Address	10. Work Unit No. (TRAIS)
SRI International 333 Ravenswood Avenue Menlo Park, CA 94025-3493	11. Contract or Grant No. 95-G-010

12. Sponsoring Agency Name and Address	13. Type of Report and Period Covered
U.S. Department of Transportation Federal Aviation Administration Office of Aviation Research Washington, DC 20591	Interim Report
	14. Sponsoring Agency Code ANE-100, ANM-100

15. Supplementary Notes

The FAA William J. Hughes Technical Center COTR is Robert H. Pursel

16. Abstract

This annual progress report describes the procedures and results of year 1 of the SRI International Phase II effort to develop engine fragment barriers for commercial aircraft and to develop a computational capability for designing fragment barriers from high-strength polymer fabrics.

The ballistic performance of various barriers of Zylon (polybenzoxazole, PBO) fabric was measured in gas gun tests using fragment simulating projectiles. Failure mechanisms and effects of multiple fabric plies and gripping mode were investigated. Absorbed kinetic energy appears to increase linearly with fabric areal density. It was found that a layer of fabric glued to the interior wall panel absorbed considerable energy at very low added weight.

To assist in model development, quasi-static penetration tests were performed with a tensile machine in conjunction with a video camera to elucidate the phenomenology and evolution of fabric failure. Tensile properties of Zylon yarn were measured at several strain rates. The framework of a fabric model was constructed and simple impacts were simulated to demonstrate efficacy.

17. Key Words	18. Distribution Statement
Aircraft engine fragments, Fragment barriers, PBO Armor, Zylon	This document is available to the public through the National Technical Information Service (NTIS), Springfield, Virginia 22161.

19. Security Classif. (of this report)	20. Security Classif. (of this page)	21. No. of Pages	22. Price
Unclassified	Unclassified	46	

TABLE OF CONTENTS

LIST OF FIGURES

LIST OF TABLES

EXECUTIVE SUMMARY

SRI International is conducting a two-phase program of research to develop lightweight barrier systems for turbine engine fragments. In Phase I, the advanced materials holding greatest promise for engine fragment barriers on aircraft were identified. The Phase II goals are to evaluate the ballistic effectiveness of fabric structures and barrier designs made from these advanced materials (high-strength polymers) and to develop a computational ability to design and evaluate barrier schemes based on material failure mechanisms and properties.

In the first year of the Phase II effort, the ballistic performance of various barrier structures of Zylon (polybenzoxazole) fabric was measured in gas gun tests using fragment simulating projectiles. Failure mechanisms and effects of multiple fabric plies and gripping mode were investigated. Absorbed kinetic energy appears to increase linearly with fabric areal density. It was found that a layer of fabric glued to the interior wall panel absorbed considerable energy at very low added weight.

To assist in model development, the tensile properties of Zylon yarn were measured at several strain rates and quasi-static penetration tests were performed with a tensile machine and video monitor to elucidate the phenomenology and evolution of fabric failure. The framework was constructed for a computational fabric model and simulated simple impact scenarios to demonstrate efficacy.

Plans for the remainder of Phase II include additional experiments (yarn tensile tests, push tests, laboratory-scale impact tests, the large-scale impact tests (at China Lake), and an extension of the computational fabric model to simulate the tests performed on Zylon fabric. By early 2000, SRI International expects to deliver to the Federal Aviation Administration a validated computational model and information on advanced materials that will enable airframers to design and evaluate lightweight engine fragment barriers.

INTRODUCTION

Over the years, several civil aircraft accidents with catastrophic consequences have occurred when fragments from in-flight engine failures damaged critical aircraft components. To reduce the probability of catastrophic consequences in future failures, the Federal Aviation Administration (FAA) established the Aircraft Catastrophic Failure Prevention Research (ACFPR) Program [1] to develop and apply advanced technologies and methods for assessing, preventing, or mitigating the effect of such failures.

In support of the ACFPR objective, SRI International is conducting a two-phase program of research aimed at developing lightweight barrier systems for turbine engine fragments. The objective of Phase I, completed in 1996, was to review the rich body of armor technology held by the Department of Defense and to identify concepts, materials, and armor designs that could lead to practical barriers to engine fragments on commercial aircraft. The findings of Phase I are documented in an FAA technical report.[2] The objective of Phase II, currently being conducted, is to capitalize on the Phase I findings by developing improved barriers and a computational barrier design capability. This report describes the experiments and computational model development work performed during the initial year of the Phase II program.

PHASE I SUMMARY.

Highly ordered, highly crystalline, high molecular weight polymers, because of their low density and high strength, were identified in Phase I as the advanced materials holding greatest promise for engine fragment barriers on aircraft. Specifically, fibers of certain aramids, polyethylenes, and poly-phenylenebenzo-bisthiazole (PBO) appear able to provide a useful measure of ballistic protection in the most weight-efficient manner. These materials can be configured as weaves, braids, knits, layups, felts, and as components of reinforced resins, providing substantial design flexibility in achieving weight-efficient barriers.

Based on these findings, a fragment barrier scheme was conceived to prevent low-energy fragments from penetrating the fuselage wall and subsequently severing control lines or damaging a second engine. The scheme consists of felts and multilayers of high-strength polymer fibers with to-be-specified spacing and boundary conditions. The barrier scheme seeks to minimize added weight and cost by replacing existing materials in the fuselage wall with dual function ballistic materials.

Gas gun experiments, in which a fragment-simulating projectile was accelerated against barriers of these fabrics confirmed that selected wovens, layups, and felts made from strong polymer fibers can absorb significant fragment energy. Furthermore, these materials appear to have sufficient flame resistance, water absorption resistance, and thermal and acoustic insulation properties to serve as building blocks for barriers. The next step is to design practical barriers from these fibers.

PHASE II PROGRAM.

SRI is now conducting the Phase II program to capitalize on these findings. Phase II consists of a semiempirical effort to evaluate the ballistic effectiveness of existing polymer fabric structures and barrier designs and to effect a modeling effort to develop a computational ability to design and evaluate barrier schemes based on material failure mechanisms and properties. The former effort is expected to result in acceptable barrier systems in the near term; the latter aims to allow, in the longer term, designs of barrier systems more optimal in terms of weight, cost, and ease of installation and removal for aircraft inspections.

By early 2000, SRI International expects to deliver to the FAA information on advanced materials that will enable airframers to design and evaluate lightweight engine fragment barriers. Specifically,

- a computational model for advanced materials insertable into the DYNA3D code,
- constitutive and failure properties for selected advanced lightweight materials,
- the special requirements of these materials when used as engine fragment barriers, and
- tailorable designs and data for advanced-material fragment barriers.

Reported here is the progress made during the first year of the Phase II effort and plans for the remainder of Phase II.

PROGRESS

Experiments were performed to investigate fragment barrier design, to assist in penetration model development, and to provide data for model verification. During this initial year, 17 gas gun tests were performed and analyzed in which 25-g (0.055-lb) or 96-g (0.21-lb) titanium alloy fragment simulator (FS) impacted targets consisting primarily of woven fabric sheets of Zylon, the PBO material that was previously identified in Phase I as most promising for fragment barriers. For some of these tests, the fabric was gripped tightly along its four edges. For other tests, the fabric was glued to one side of a sample of an airplane's interior wall panel.

To assist in developing computational failure models, the impacted targets were examined to determine the failure mechanisms of fabrics and yarns, measure geometrical details of the Zylon fabric and the tensile properties of individual yarns over a range of strain rates, and design and perform a quasi-static penetration test (the "push test") that allows a fragment or FS to be slowly pushed through a target to observe the evolution of damage during penetration. Following is a brief description of the procedures and the results.

A variety of Zylon materials was provided by Toyobo Company, Ltd., of Osaka, Japan. Included were weaves made of nominally 500-denier (0.55 mg/cm) Zylon yarn, with meshes ranging from 30 x 30 to 40 x 40 yarns/in. unwoven Zylon yarn, and Zylon felt. (The 45 x 45 yarns/in. fabric that was previously tested was not available.)

FRAGMENT IMPACT TESTS.

A gas gun was used to impact a FS into targets containing one or more plies of Zylon weaves. The experimental method is described in detail in reference 2. Figure 1 shows the experimental setup for the tests, along with the dimensions of both the 25- and 96-g FS. Minor improvements were made in the design of the sabot stopping fixture to minimize the rotation of the FS and the resultant pitch at impact. A high-speed camera was used (at ≈ 20,000 frames/s) to record the motion of the FS before and after impact, allowing calculations, for the cases of full penetration, of the energy absorbed by the target.

TESTS WITH TIGHTLY GRIPPED ZYLON FABRIC. To investigate the effect of boundary conditions on ballistic performance, a series of gas gun tests were first performed in which one or more of the Zylon fabric plies were tightly gripped along its four edges to take full advantage of their fiber tensile strength. Figure 2(a) shows the details of the scheme employed for tightly clamping the square cross-shaped fabric targets to minimize slipping during the test. Table 1 is a matrix of parameters for the gas gun tests (and two previously performed Zylon fabric tests).

Effect of Fabric Mesh. Tests were performed with the 25-g FS at impact velocities of ≈80 m/s (262 ft/s) into fabrics of different meshes (Tests 13, 20, 24, 25, and 26) to compare the ballistic performance. Results are shown in table 1 and figures 3 and 4 for Zylon fabrics with meshes that vary from 30 x 30 to 45 x 45 yarns/in. A monotonic increase in energy absorbed by the Zylon fibers of tighter mesh (and therefore larger areal density)—from ≈32 J (24 ft-lbs) for the 30 x 30 mesh to ≈65 J (48 ft-lbs) for the 30 x 30 mesh—which is equivalent to a linear increase with target areal density was observed. Thus, the specific energy absorbed (SEA) of the different Zylon fabric meshes is roughly constant. The variation observed (roughly ± 12%) was not monotonic with mesh density and was likely due to material variability or a slight variation in impact conditions.[1]

Effect of Number of Fabric Plies. Two tests were performed (Tests 29 and 32) with the 96-g FS at impact velocities of ≈80 m/s (262 ft/s) into multiple layers of the Zylon 40 x 40 yarns/in. fabric to examine the effects of multiple layers on the specific energy absorbed (SEA). Table 1 and figure 4 show the results of these tests along with results of the previous tightly gripped, single- and multiple-ply Zylon fabric tests.

The SEAs for all of these tests fall within a band of 3000 J/g/cm^2 (1080 ft-lbs/lb/ft^2) ± 20%, which implies that the energy absorbed is approximately proportional to the number of plies. However, this is a preliminary result only. The 96-g FS has a cross-sectional area 62.5%

[1] It is anticipated that some of the variation of the SEA is caused by variation in the experimental conditions (such as pitch and yaw of the FS at impact and initial gripping traction on the fabric target) and some by material variability (as discussed later, there is a significant variation in the denier, or linear density, of the individual yarns that make up the fabric). Because only one or two tests were performed for the different fabric meshes, it is not known what the typical SEA variability is for a particular fabric impacted at the same velocity by the same FS.

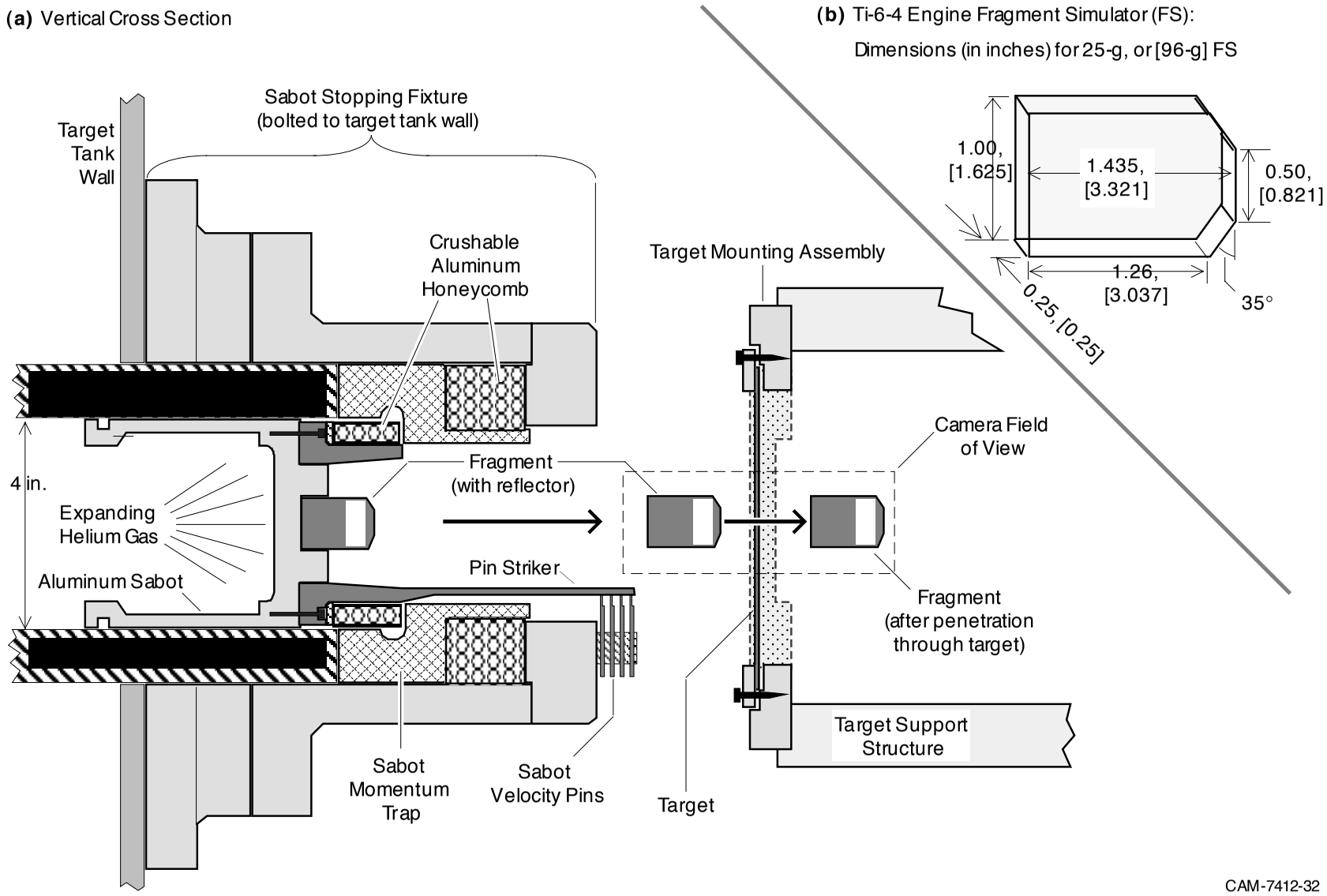

FIGURE 1. EXPERIMENTAL SETUP FOR GAS GUN IMPACT TESTS TO EVALUATE POTENTIAL ENGINE FRAGMENT BARRIERS (Details of the target mounting and clamping scheme are shown in figure 2.)

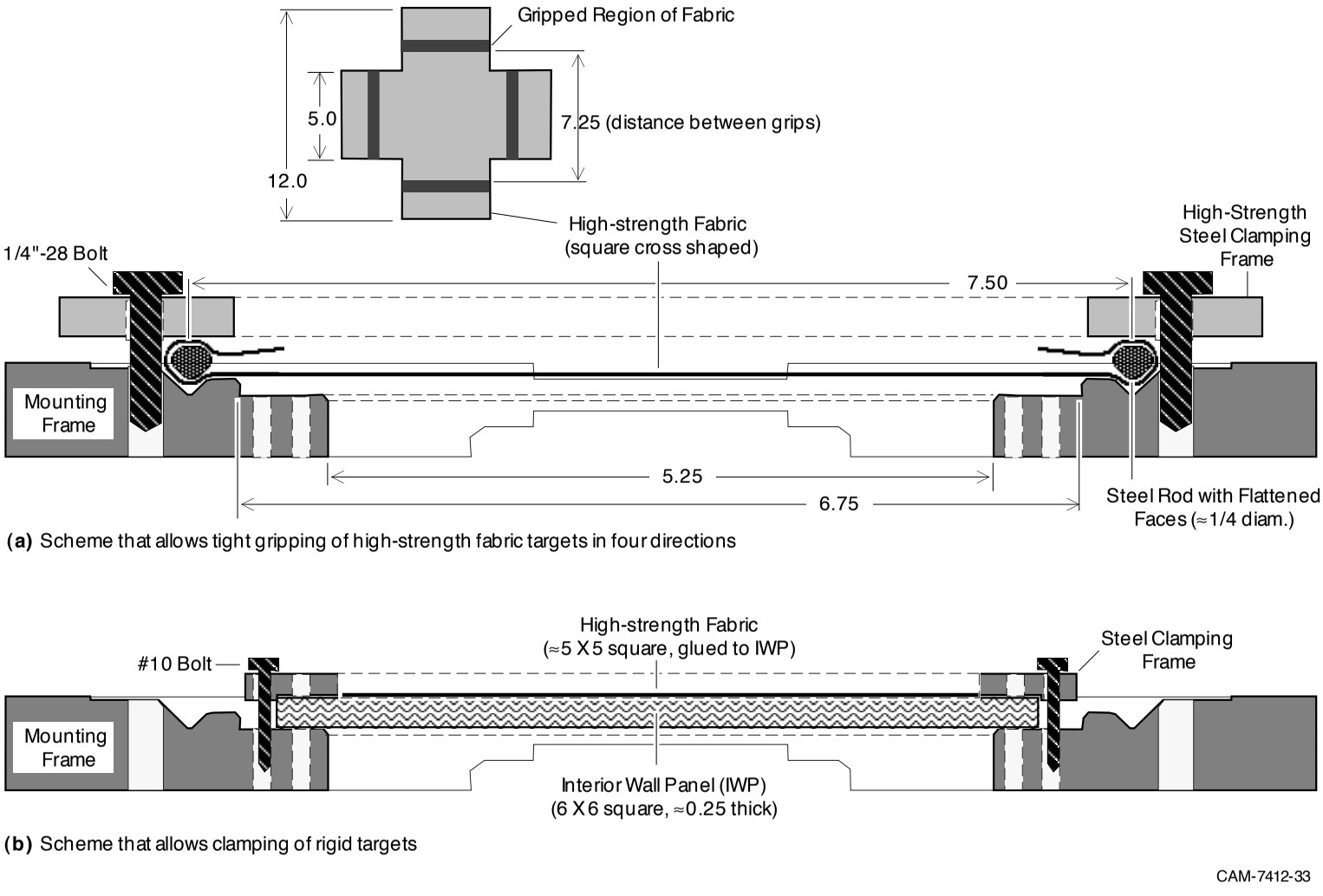

FIGURE 2. TARGET MOUNTING AND CLAMPING SCHEMES USED IN GAS GUN IMPACT EXPERIMENTS TO EVALUATE POTENTIAL ENGINE FRAGMENT BARRIERS.
(All dimensions in inches; fragment simulator impacts from top of drawing.)

TABLE 1. GAS GUN IMPACT TESTS WITH TARGETS OF ZYLON FABRICS TIGHTLY GRIPPED ON FOUR EDGES

Test No.[a]	Target				Areal Destiny (g/cm^2)	FS[b]: Before Impact			FS: After Penetration				Specific Energy Absorbed[c] ($J/g/cm^2$)
	Material(s)	Mesh (Yarns/in.)	Thickness per Ply (in.)	No. of Plies		Mass (g)	Velocity (m/s)	Kinetic Energy (J)	Velocity (m/s)	Kinetic Energy (J)	Kinetic Energy Lost (J)	Kinetic Energy Lost (%)	
13	Zylon	45 x 45	≈0.011	1	0.0219	25	78	76	29	10.5	65.5	86	2990
19[d]	Zylon	45 x 45	≈0.011	2	0.0438	25	113	160	64	51.5	108.5	68	2477
20	Zylon	30 x 30	≈0.006	1	0.0130	25	79	78	61.5	47.5	30.5	39	2346
26	Zylon	30 x 30	≈0.006	1	0.0130	25	82.5	85	63	49.5	34.5	41	2654
25	Zylon	35 x 35	≈0.0075	1	0.0158	25	77.5	75	59	43.5	37.5	42	2373
24	Zylon	40 x 40	≈0.009	1	0.0185	25	79	78	49.5	30.5	48.5	61	2622
29	Zylon	40 x 40	≈0.009	4	0.0740	96	79	300	27.5	36.5	263.5	88	3560
32	Zylon	40 x 40	≈0.009	6	0.111	96	79	300	Did not Penetrate[e]		300.0	100	2702
23	Zylon	30 x 30	≈0.006	1	0.0130	25	80	80	35.5[f]	20[f]	60.0	75	——
	UHMW Polyethylene Felt		≈0.13	1	+0.0309								
22	Zylon	30 x 30	≈0.006	1	0.0130	25	82	84	Did not Penetrate[g]		84.0	100	——
	UHMW Polyethylene Felt		≈0.13	2	+0.0618								

a Tests 13 and 19 were performed and reported during the previous reporting year.

b Fragment simulator.

c Specific energy absorbed (SEA) is defined as energy absorbed per unit areal density.

d Data from this test are questionable due to the excessive pitch, debris from the aluminum honeycomb momentum trap traveling ahead of the impactor, and some PBO fibers from the back (22° orientation) layer breaking at the corner of the clamping rod, thus likely reducing the absorbed kinetic energy.

e The impactor penetrated only the first of the six layers.

f The impactor did not penetrate the felt; however, the impactor, surrounded by the felt layer, completely penetrated the fabric.

g Only partial penetration was obtained in this test. The impactor, surrounded by the felt, remained lodged in the hole in the fabric.

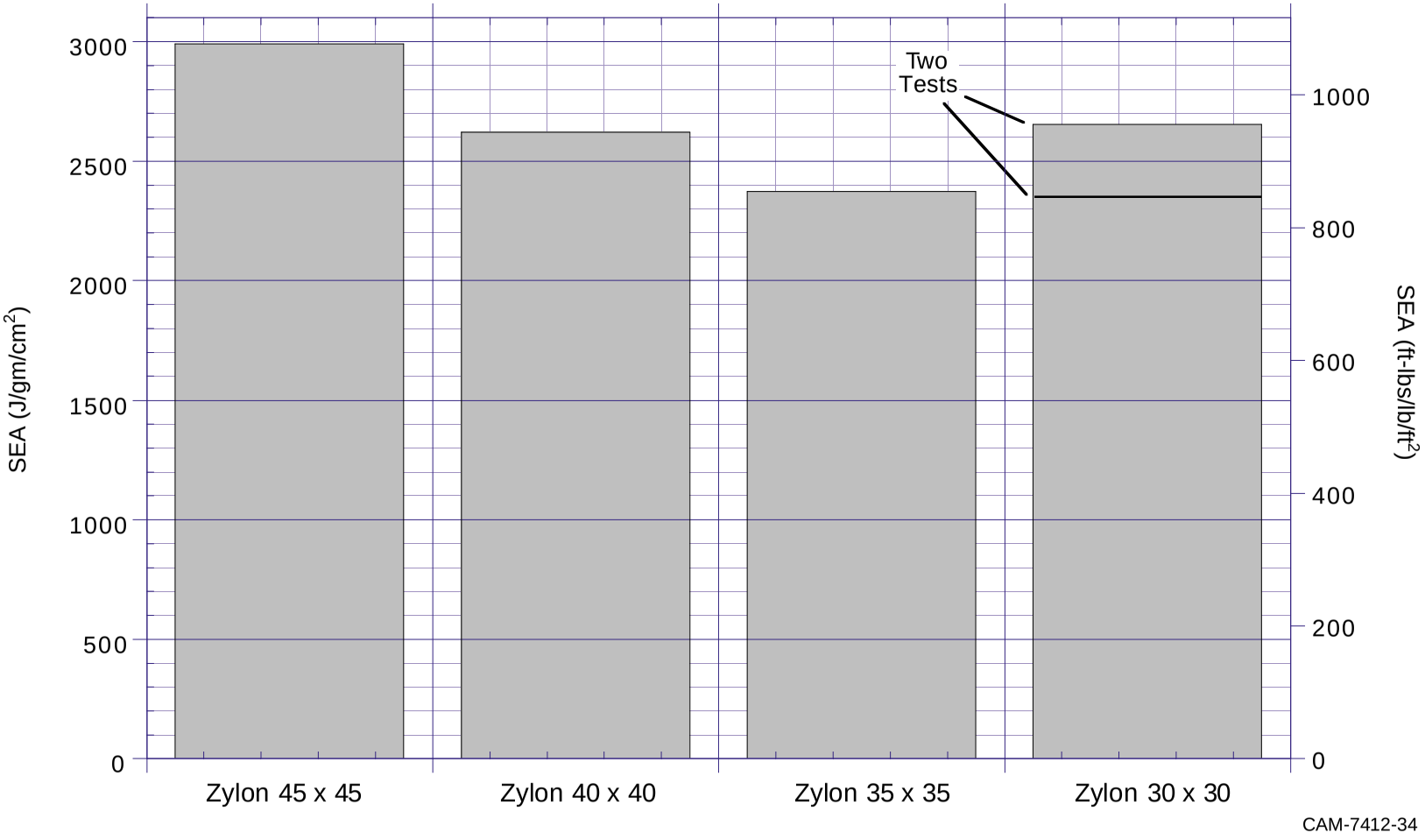

FIGURE 3. SPECIFIC ENERGY ABSORBED (SEA) FOR SINGLE PLIES OF ZYLON FABRIC PENETRATED BY 25-g FRAGMENT SIMULATOR AT ≈80 m/s (SEA is defined as the energy absorbed per unit area density.)

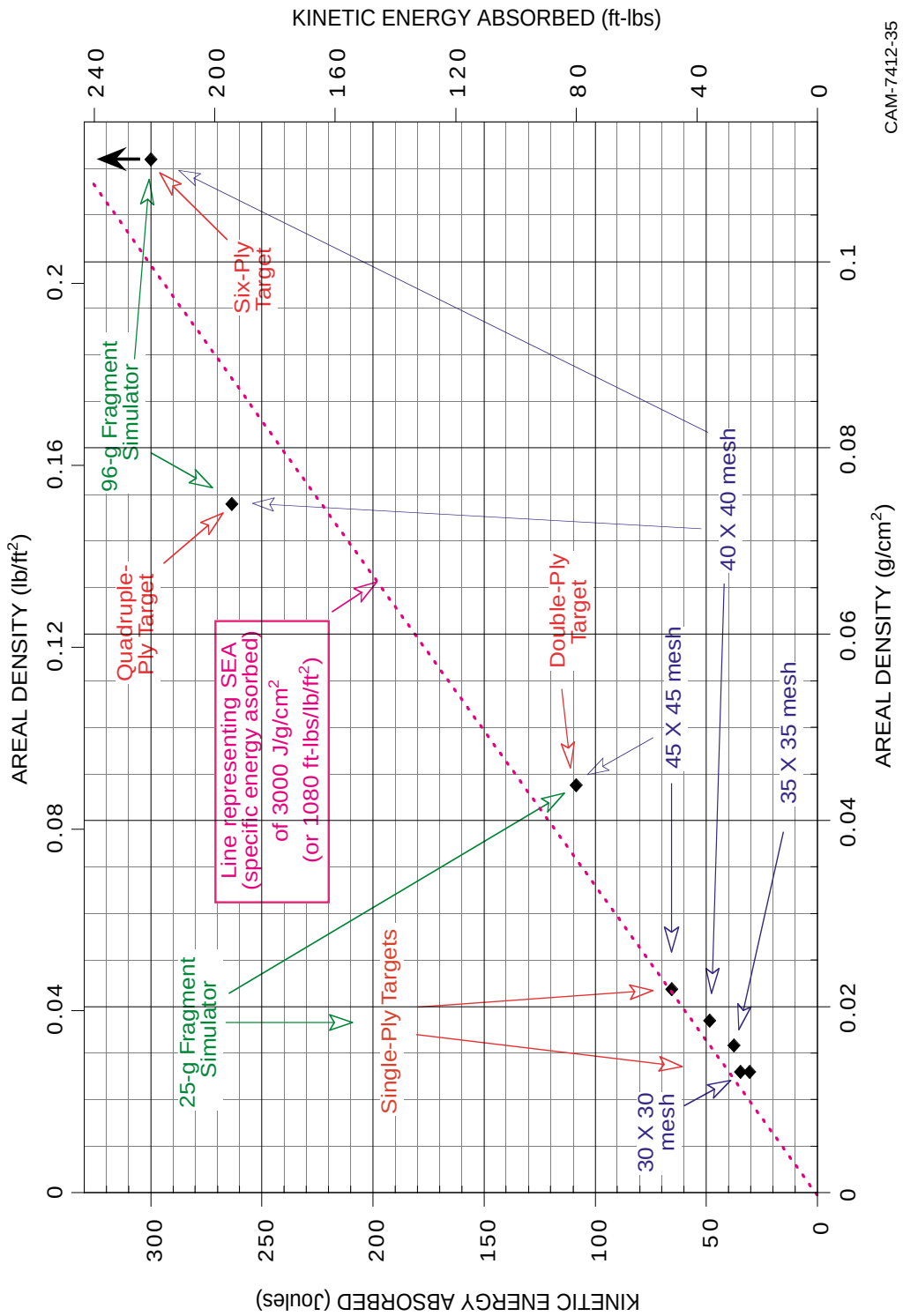

FIGURE 4. KINETIC ENERGY ABSORBED BY ZYLON FABRIC TARGETS IMPACTED BY Ti-6-4 FRAGMENT SIMULATOR. (Note: all tests resulted in full penetration except for the test with a six-ply target, whose plotted value represents a lower bound.)

greater than the 25-g FS, so one would expect the SEA to be higher for the larger impactor because it would need to break more yarns to penetrate the target. Also, the fact that the same impactor traveling at the same velocity penetrated only the first ply of the six-ply target after having penetrated all four plies of the four-ply target suggests a more complex behavior—that an N-ply target does not behave as N single-ply targets. Additional full-penetration tests are planned with multiple-ply targets to yield a more definitive determination of the effect of multiple-ply targets.

Effect of High-Strength Felt. Two tests were also performed (Tests 22 and 23) in which one or two sheets of Spectra (UHMW polyethylene) felt were placed on the impact side of a single-ply 30 x 30 Zylon fabric (the Zylon was tightly gripped on four edges as before, but the felt was only taped along its edges to the Zylon) and impacted the targets with the 25-g FS at ≈80 m/s (262 ft/s). These were preliminary tests to examine the effectiveness of high-strength felt as a fragment barrier component. Provided that a fragment did not penetrate the felt layers, the felt might blunt the sharp edges of a fragment impactor, increase the effective cross-sectional area of the fragment, and increase the drag of the fragment; all effects that would increase the energy absorbed in penetrating the fabric target.

The results were promising. In both tests, the FS did *not* penetrate the felt layer(s) but instead remained wrapped in the felt as the FS attempted to penetrate the target. For the case with the single felt layer (Test 23), the FS, surrounded by the felt, completely penetrated the Zylon fabric target, but the target absorbed roughly twice the energy absorbed in similar tests (Tests 20 and 26) without the felt. For the case with two felt layers (see figure 5), the FS, encased in the felt, passed partway through a hole created in the fabric but was stopped before the felt-wrapped FS could completely exit the hole.

Further testing is planned to confirm the effectiveness of high-strength felt as a fragment barrier component. Specifically, it is necessary to determine whether additional layers of the woven fabric with the same area density as the felt layers would be just as effective as the felt layers in increasing the energy absorbed during a fragment impact.

TESTS WITH THE ZYLON FABRIC GLUED TO INTERIOR WALL PANELS. Although gripping the fabric tightly along all four edges takes advantage of the high-fiber strength in a fabric barrier, it may not be practical (because of weight considerations) to use strong, rigid metal fixtures for tight gripping. An investigation is being conducted with other fabric gripping methods that are more practical but still exploit the high-fiber strength.

Several designs were considered and the design chosen for the gas gun tests was gluing the fabric to the impact side of an airplane's interior wall panel (IWP). Gluing would be one of the simplest ways to hold the fabric barriers and might involve the least amount of additional weight. Because there is no gripping frame, the weight of the adhesive is the only additional weight.

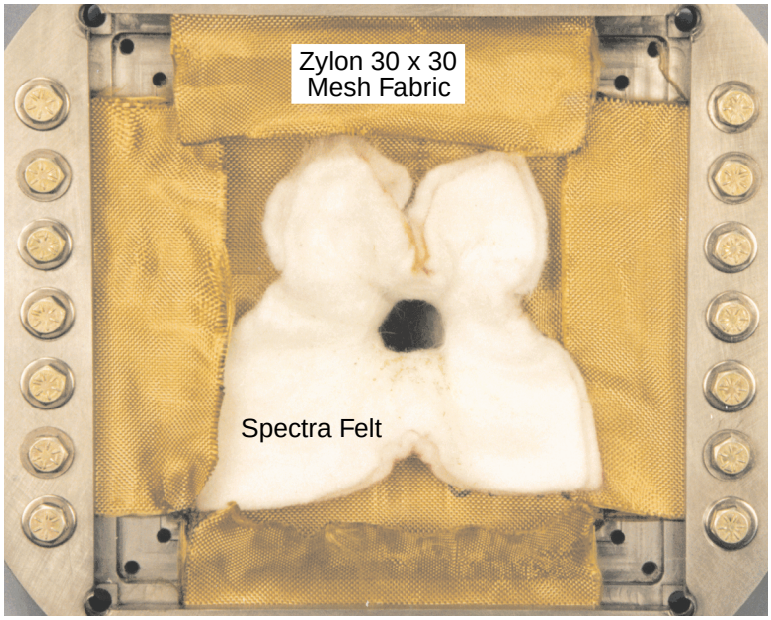

(a) Impact Side

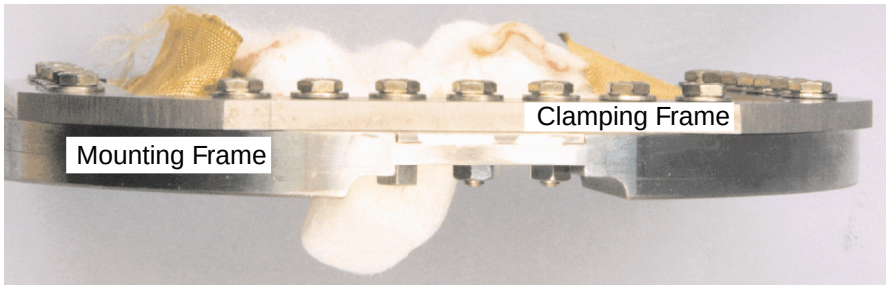

(b) Edge View

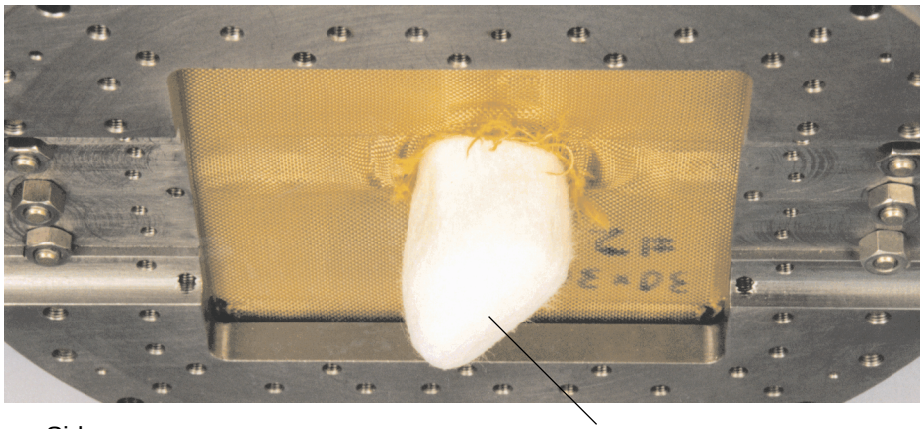

(c) Rear Side

CAM-7412-36

FIGURE 5. POSTTEST PHOTOGRAPHS OF TEST 22: 25-g FRAGMENT SIMULATOR INTO TWO LAYERS OF SPECTRA FELT OVER ZYLON FABRIC
(Impact velocity was 82 m/s.)

A matrix of the test parameters and some ballistics results appear in table 2. The IWP material used was provided by United Airlines. The material is a lightweight, rigid sandwich structure 6.35 mm (0.25 in.) thick, consisting of a plastic honeycomb core bonded on both sides to thin, two-dimensional, fiber-reinforced resin sheets. Many different IWP materials and structures are used in airplanes. No attempt was made to characterize any particular IWP but instead to use it as a representative example of an IWP to which could be glued the high-strength fabrics and to test the effectiveness of this fabric holding scheme.

For the gas gun impact tests, the IWP was cut into 15.2-cm (6-in.) squares and was held in place between the mounting and clamping frames in the manner shown in figure 2(b). Little clamping pressure could be used, however, because the IWP collapses at relatively low pressures. The Zylon fabric plies were glued onto the impact side of the IWP using Shell Epon 815 adhesive. A roughly 5-in. square of Zylon was glued to the 6-in.-square IWP, which meant that the Zylon did not extend into the clamped region. An areal density of ≈0.01 g/cm^2 (0.02 lb/ft^2) of adhesive per ply of fabric appeared to completely wet the woven yarns and led to little or no debonding of the fabric from the IWP during impact. When the amount of adhesive was reduced to ≈0.006 g/cm^2 (0.012 lb/ft^2) per ply of fabric, complete or partial debonding occurred during impact (Tests 35 and 36).

The energy absorbed by the IWP alone during an impact at ≈80 m/s (262 ft/s) by the 25-g and 96-g FS was determined. Two tests (Tests 27 and 33) yielded complete penetration with no damage to the IWP except in the impact zone (figures 6(a) and 6(b) are posttest photographs from Test 27). The energy absorbed was 35 J (26 ft-lbs) for the 25-g FS and 47 J (35 ft-lbs) for the 96-g FS; the variance is reasonable considering that the cross-sectional area of the 96-g FS is larger than that of the 25-g FS. The SEA of the IWP for the 25-g FS was 147 J/g/cm^2 (53 ft-lbs/lb/ft^2), which is somewhat less than the 185 J/g/cm^2(67 ft-lbs/lb/ft^2) which was previously measured for the aluminum fuselage skin.

Three tests were then performed with a single ply of Zylon glued to the impact side of an IWP. In the two ≈80 m/s (262 ft/s) tests (Test 28 with Zylon 45 x 45 mesh and Test 30 with Zylon 40 x 40 mesh); although some of the Zylon yarns in the impact zone were severed and structural damage was observed in the IWP far from the impact zone (near the edge of the panels at azimuthal angles of 0°, 90°, 180°, and 270°, as shown in figures 6(c) and 6(d)), the targets did not allow the 25-g FS to penetrate completely. For these tests, the energy absorbed (as shown in table 2) was about 75 J (55 ft-lbs), more than double the energy absorbed by the bare IWP. The SEA for the entire target (including the IWP, Zylon fabric, and adhesive) was ≥ 280 J/g/cm^2 (100 ft-lbs/lb/ft^2) or at least double that of the IWP alone.[2] The additional SEA caused by the

[2] Because complete penetration was not achieved in these tests, the values obtained are only lower bounds on the actual SEA values.

TABLE 2. GAS GUN IMPACT TESTS USING ZYLON FABRICS GLUED TO IMPACT SIDE OF INTERIOR WALL PANELS

Test No.	Target Components: Plies	Material	Size (in. sq.)	Mass (g)	Areal Density (g/cm^2)	FS[a]: Before Impact: Mass (g)	Velocity (m/s)	K.E. (J)	Impact Results	FS: After Impact: Velocity (m/s)	K.E. (J)	K.E. Lost (J)	(%)	Specific Energy Absorbed (SEA)[b] (J/g/cm^2)	Additional SEA[c] (J/g/cm^2)
27	1	IWP[d]	6.00	55.3	0.238	25	76	72	Penetration	54.5	37	35	49	147	———
28	1	IWP	6.00	53.4	0.230				No Penetration: impactor rebounded after severing Zylon fibers in impact region and damaging IWP near edges at 0°, 90°, 180°, and 270°; negligible debonding of fabric from IWP						
	1	Zylon 45 x 45	5.13	3.7	0.022										
		Adhesive[e]	5.13	1.6	0.009										
		Total	——	58.7	0.261	25	76.5	73		——	0	73	100	≥ 280	≥ 1211
30	1	IWP	6.00	55.1	0.237				No Penetration: impactor rebounded after severing Zylon fibers in impact region and damaging IWP near edges at 90° and 270°;negligible debonding of fabric from IWP						
	1	Zylon 40 x 40	4.93	2.9	0.018										
		Adhesive	4.93	1.6	0.010										
		Total	——	59.6	0.266	25	78.5	77		——	0	77	100	≥ 290	≥ 1462
31	1	IWP	6.00	54.9	0.236				Penetration: damage to IWP plate limited to region in and around impact zone; negligible debonding of fabric from IWP						
	1	Zylon 40 x 40	4.93	2.9	0.018										
		Adhesive	4.93	1.6	0.010										
		Total	——	59.4	0.265	25	96	115		66.0	54	61	53	229	895
33	1	IWP	6.00	54.3	0.234	96	79	298	Penetration	72.5	251	47	16	201	———
34	1	IWP	6.00	54.7	0.236				No Penetration: impactor severely bent IWP along 0°-180° axis, forcing it through 5.25-in.-square mounting frame; no failure in fabric layer and only minor debonding from IWP						
	4	Zylon 40 x 40	4.93	11.9	0.076										
		Adhesive	4.93	5.7	0.036										
		Total	——	72.3	0.348	96	79.5	303		——	0	303	100	———	———
35	1	IWP	6.00	54.4	0.234				No Penetration: impactor rebounded after forcing severely bent (on 90°-270° axis) IWP through mounting frame and fabric layer (did not fail but totally debonded) into hole in IWP						
	1	Zylon 40 x 40	4.93	2.8	0.018										
		Adhesive	4.93	1	0.006										
		Total	——	58.2	0.258	96	79.5	303		——	0	303	100	———	———
36	1	IWP	6.00	54.2	0.233				No Penetration: impactor rebounded after forcing severely bent (on 90°-270° axis) IWP partway through mounting frame; fabric layers did not fail but partially debonded.						
	2	Zylon 40 x 40	4.93	5.6	0.036										
		Adhesive	4.93	1.9	0.012										
		Total	——	61.7	0.281	25	108	146		——	0	146	100	———	———

[a] Fragment simulator.

[b] The energy absorbed per unit areal density of the entire target (including the IWP, fabric, and adhesive).

[c] Increase of the energy absorbed due to the addition of the fabric (as compared to the same impact conditions without the fabric) divided by the unit areal density of the added fabric and adhesive.

[d] Interior wall panel provided by United Airlines ("Gillfab 4122A Faceside, 250 x 48 x 96 .020/.020, 3/16 - 3.0 lbs core, SHE 2904C0250-202REVNC, LOT 30144 mfg. 11/9/95")

[e] Adhesive used was Shell Epon 815.

presence of the fabric—the increase in energy absorbed due to the addition of the fabric (as compared to the same impact conditions without the fabric) divided by the unit areal density of the added fabric and adhesive—was ≥ 1200 J/g/cm^2 (432 ft-lbs/lb/ft^2).

A higher impact velocity (Test 31, at 96 m/s or 315 ft/s) resulted in complete penetration of the fabric and IWP. The energy absorbed was 61 J (45 ft-lbs), the SEA for the entire target was 229 J/g/cm^2 (82 ft-lbs/lb/ft^2), and the additional SEA caused by the presence of the fabric was 895 J/g/cm^2 (322 ft-lbs/lb/ft^2). Less energy was absorbed in complete penetration of the target than in the two tests at lower velocities in which the FS was stopped. The difference is attributable to the greater structural damage sustained by the IWP in the case of no penetration (see figures 7(a) and 7(b)). Apparently the FS perforated the fabric and IWP so quickly that insufficient impulse was delivered to the panel to cause the type of structural damage seen at lower impact velocities where the fabric was not perforated. Although all (or almost all) of the absorbed energy in the higher-velocity test went into perforating the fabric and IWP, most of the energy in the lower-velocity tests went into structural damage of the IWP.

Additional tests were performed at significantly higher impact kinetic energies (Tests 34 through 36, as shown in table 2) using one to four layers of Zylon fabric glued to the IWP. In all three tests, the FS did not penetrate the target or any of the Zylon layers, but the 6-in.-square IWP experienced enough structural damage (primarily by bending on the 0°-180° or 90°-270° axis as seen in figures 7(c) and 7(d)) that it was forced completely or partially through the 5.25-in.-square hole in the mounting frame.

The maximum amount of energy that can be absorbed by an IWP panel before it experiences structural failure is strongly dependent upon the panel material, panel size, and the boundary conditions (how it is attached to the fuselage). For a 6-in. square of this particular IWP, clamped along its periphery, enough energy to structurally fail the IWP (which, in this case, means enough bending to allow it to pass through a 5.25-in.-square window) can be attained by gluing only a single ply of Zylon fabric to the IWP. Larger panels and different boundary conditions would certainly increase the minimum failure energy and perhaps even change the failure mode. The mission is not to characterize the ballistic properties of IWPs, but to recognize that using this approach of gluing high-strength fabric barriers to an IWP will require an understanding of the IWP failure dynamics.

In comparing the gripping methods, Test 31, with the Zylon glued to the IWP, can be compared with Test 24 (see table 1), with the same FS impacting the same Zylon fabric, where the fabric is tightly gripped on four edges. Because the edges of the fabric did not debond from the IWP in Test 31, the boundary conditions are similar to that of Test 24 in that the yarns are effectively tightly gripped at their ends. One difference is that for Test 24 the gripped ends were ≈7.5 in. apart (the distance between opposite clamping rods, as shown in figure 2(a)) while for Test 31 the gripped ends were between ≈0.75 to 1.5 in. apart (the dimensions of the perforated fabric and damaged IWP).

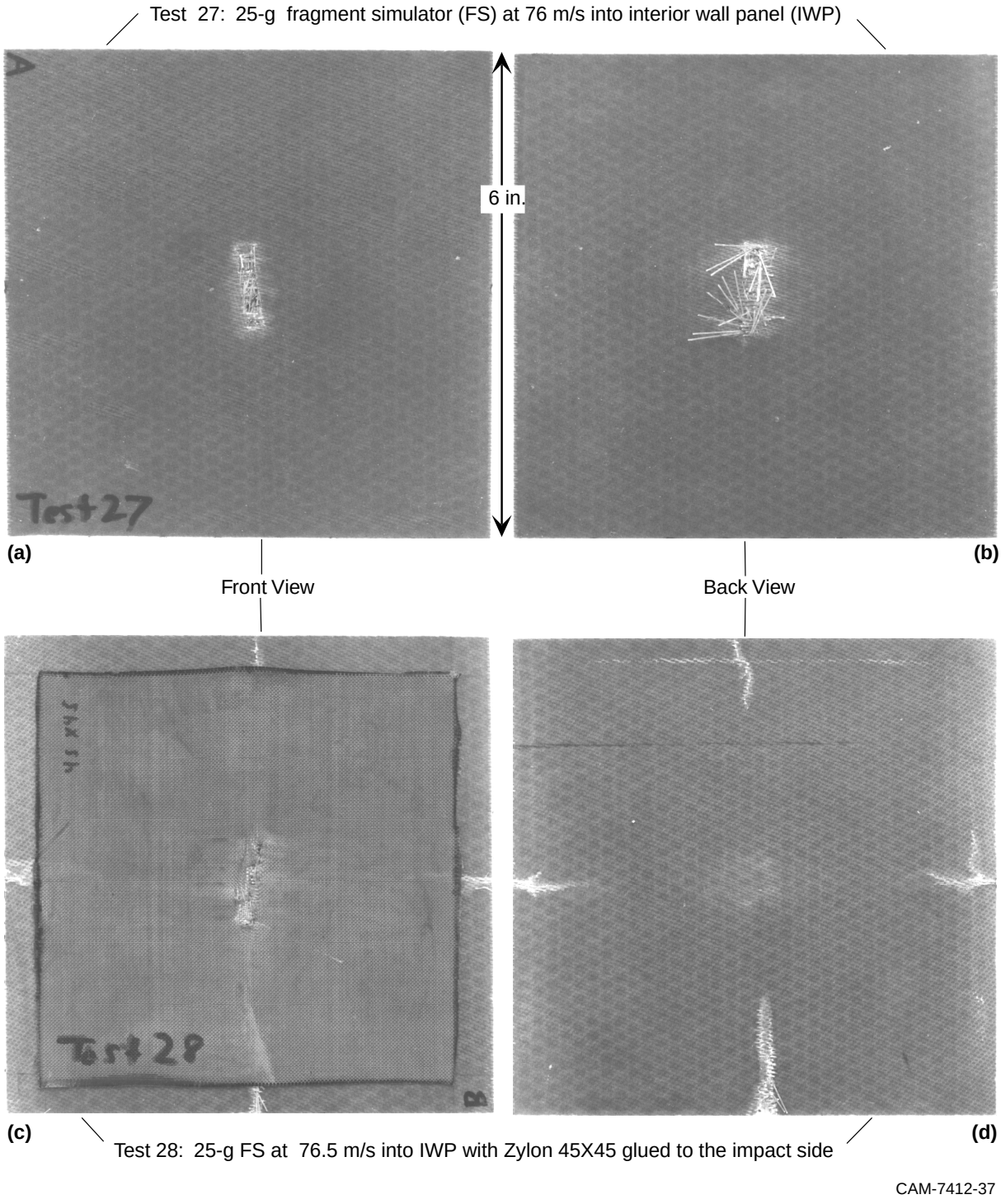

FIGURE 6. RECOVERED TARGETS FROM GAS GUN IMPACT TESTS 27 AND 28

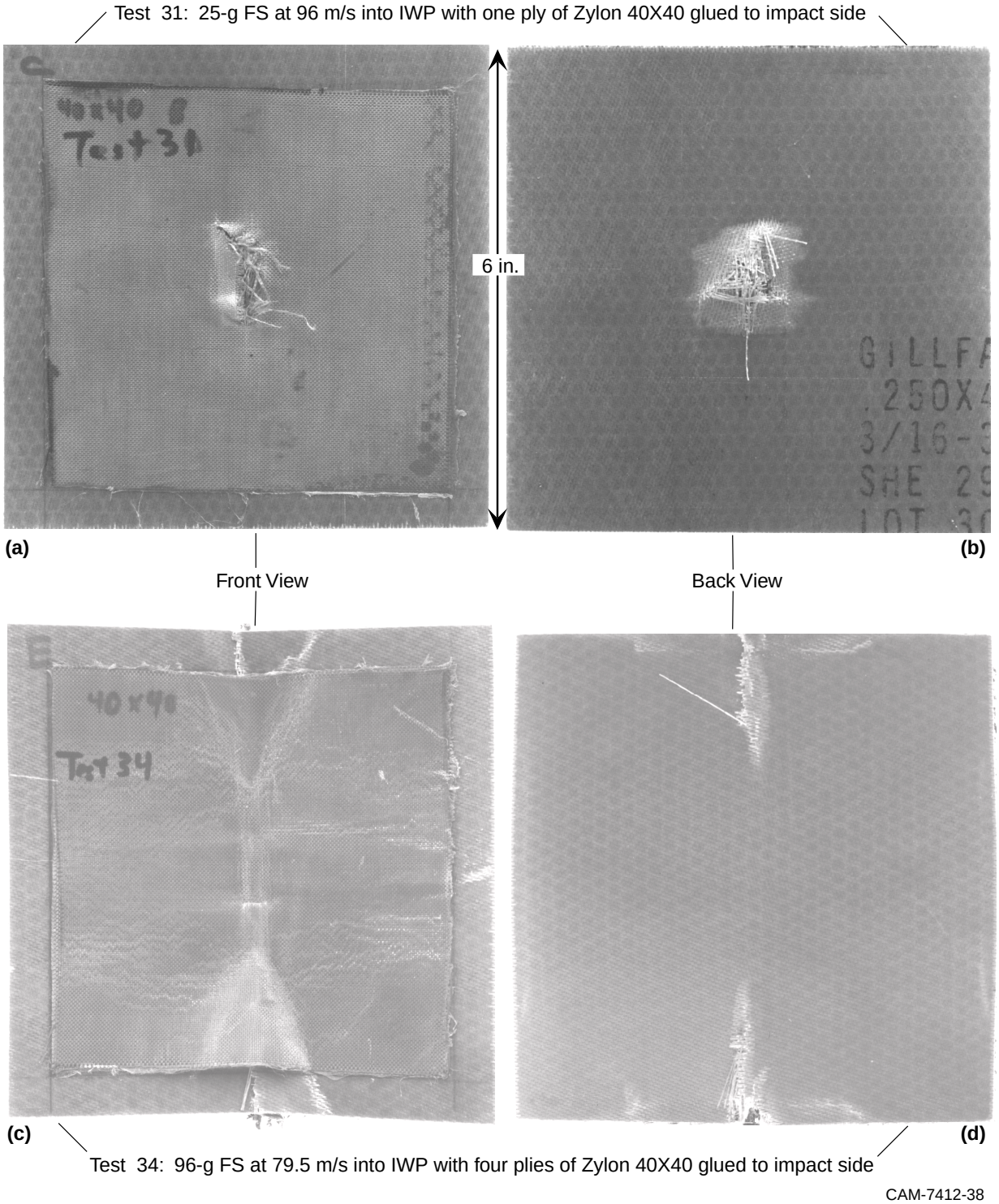

FIGURE 7. RECOVERED TARGETS FROM GAS GUN IMPACT TESTS 31 AND 34

Because the amount of energy that a yarn can absorb by stretching before failure is proportional to the length of the yarn, a fabric with a longer distance between gripped ends would be expected to absorb more energy prior to failure. That is just what is seen when comparing Tests 24 and 31. The energy absorbed by the fabric is 48.5 J (36 ft-lbs) for Test 24 but only 26 J (19 ft-lbs) were needed to perforate the fabric in Test 31 (in addition to the 35 J or 26 ft-lbs required to perforate the IWP). Although these tests cannot be compared quantitatively (because of the presence of adhesive and IWP in one of the tests), the results emphasize the importance of boundary conditions in energy absorption of high-strength fabrics; larger target dimensions—in particular larger stretchable regions (i.e., regions between grips that are not glued to a rigid panel)—allow for greater energy absorption. Additional tests are planned to examine modifications to the methods of attaching the fabric to the IWP that would increase the effective ungripped length and hence enhance the energy absorption. These modifications include gluing the fabric around the periphery but not near the impact zone and gluing it to the back (nonimpact) side of the IWP.

The conclusion from these tests is that gluing the fabric to the IWP is easy to do, adds relatively little weight, and can substantially increase the energy absorbed by an impacting fragment as compared to that absorbed by the IWP alone. However, in considering this fabric barrier holding method, one would need to consider, in addition to the energy needed to perforate the fabric liner, the energy needed to cause structural failure in the IWP and the severity of the consequences of such failure (i.e., is it better to have a large panel of IWP moving inward into the fuselage at a low velocity or a single hard fragment move through at a much higher velocity).

TESTS TO AID MODEL DEVELOPMENT.

To assist the development, calibration, and verification of computation models for the deformation and failure of high-strength fabric for application to engine fragment barriers and to measure relevant fabric failure model properties, the following tasks were accomplished.

- Examined the woven Zylon fabrics microscopically to determine the shape and dimensions of their constituent Zylon yarn.
- Examined yarns removed from the Zylon fabrics and determined the degree of crimping of the yarns in the fabrics.
- Designed a method for conducting tensile tests on individual yarns over a range of strain rates and began a series of tensile tests on Zylon yarns removed from various fabrics as well as on unwoven Zylon yarns.
- Designed and implemented a new test in which a rigidly held fragment or FS is slowly pushed into high-strength fabric targets of various configurations and boundary conditions while recording the load and stroke and, if desired, take photographs of the deforming target. A preliminary test series was recently completed.

Results of these tasks will now be discussed in detail.

EXAMINATION OF THE ZYLON FABRICS. Table 3 shows the high-strength fabric materials that were obtained for use during this reporting period. They include a number of Zylon 2-D weaves with mesh size varying from 30 x 30 to 45 x 45 in., one Spectra and two Zylon felts and two spools of unwoven Zylon yarn.

First examined were the woven fabrics. The Zylon weaves consist of nominally 500-denier yarns, each of which is made up of several hundred individual filaments or fibers (preliminary scanning electron microscope (SEM) and scanning laser microscope pictures showed these filaments to be roughly cylindrical with a diameter of 8 μm or $3x10^{-4}$ in.). Two arrays of yarns, the fill yarns and the warp yarns, are oriented perpendicularly to each other. The fill yarns are relatively straight, but the warp yarns weave over and under the fill yarns and are therefore somewhat bent or crimped, the extent of crimping being a function of the tightness of the weave.

TABLE 3. HIGH-STRENGTH FABRIC MATERIALS OBTAINED FOR FRAGMENT BARRIER PROGRAM

Trade Name[a]	Material [b]	Fabric Structure			Approximate Thickness		Areal Density	
		Type	Mesh (yarns/in.),	Denier[c] (g/9 km)	(in.)	(mm)	(g/cm^2)	(lb/ft^2)
Zylon	PBO-AS	2-D Weave,	45 x 45,	500	0.011	0.27	0.0219	0.0449
Zylon	PBO-AS	2-D Weave,	40 x 40,	500	0.009	0.23	0.0185	0.0378
Zylon	PBO-AS	2-D Weave,	35 x 35,	500	0.0075	0.19	0.0158	0.0324
Zylon	PBO-AS	2-D Weave,	30 x 30,	500	0.006	0.15	0.0130	0.0266
Spectra	UHMW Polyethylene	Felt,	—	—	0.14	3.6	0.0309	0.0633
Zylon	PBO-AS	Felt (No. 1),	—	1.5	0.13	3.4	0.0104	0.0213
Zylon	PBO-AS	Felt (No. 2),	—	1.5	0.009	2.4	0.0080	0.0164
Zylon	PBO-AS	Unwoven Yarn,	—	500	—	—	—	—
Zylon	PBO-HM	Unwoven Yarn,	—	500	—	—	—	—

[a] Zylon was supplied by Toyobo Co., Ltd., in Osaka, Japan; Spectra was provided by Spectra Performance Materials, Petersburg, VA.

[b] PBO (polybenzbisoxazole) is manufactured in two types, AS and HM, with somewhat different properties; UHMW means ultra-high molecular weight.

[c] Denier denotes linear density in terms of grams per 9 kilometers. Nominal denier values shown are for the yarns except in the case of the felts where the denier values are for the individual filaments.

To enable explicit modeling of the yarns in a woven fabric, the size, shape, and relative locations of the yarns in the fabric need to be determined. Because it is difficult to cut a section of fabric without unraveling the filaments near the cut, a small piece of each Zylon fabric was potted into a plastic potting compound. Sections perpendicular to the axial directions of the warp and the fill yarns were then cut, ground, and polished and a stereomicroscope was used to examine the cross sections.

Photomicrographs for two of the fabrics, the 30 x 30 mesh and the 45 x 45 mesh, are shown in figure 8. For both the fill and warp yarns, the shape of the cross sections is different for the two

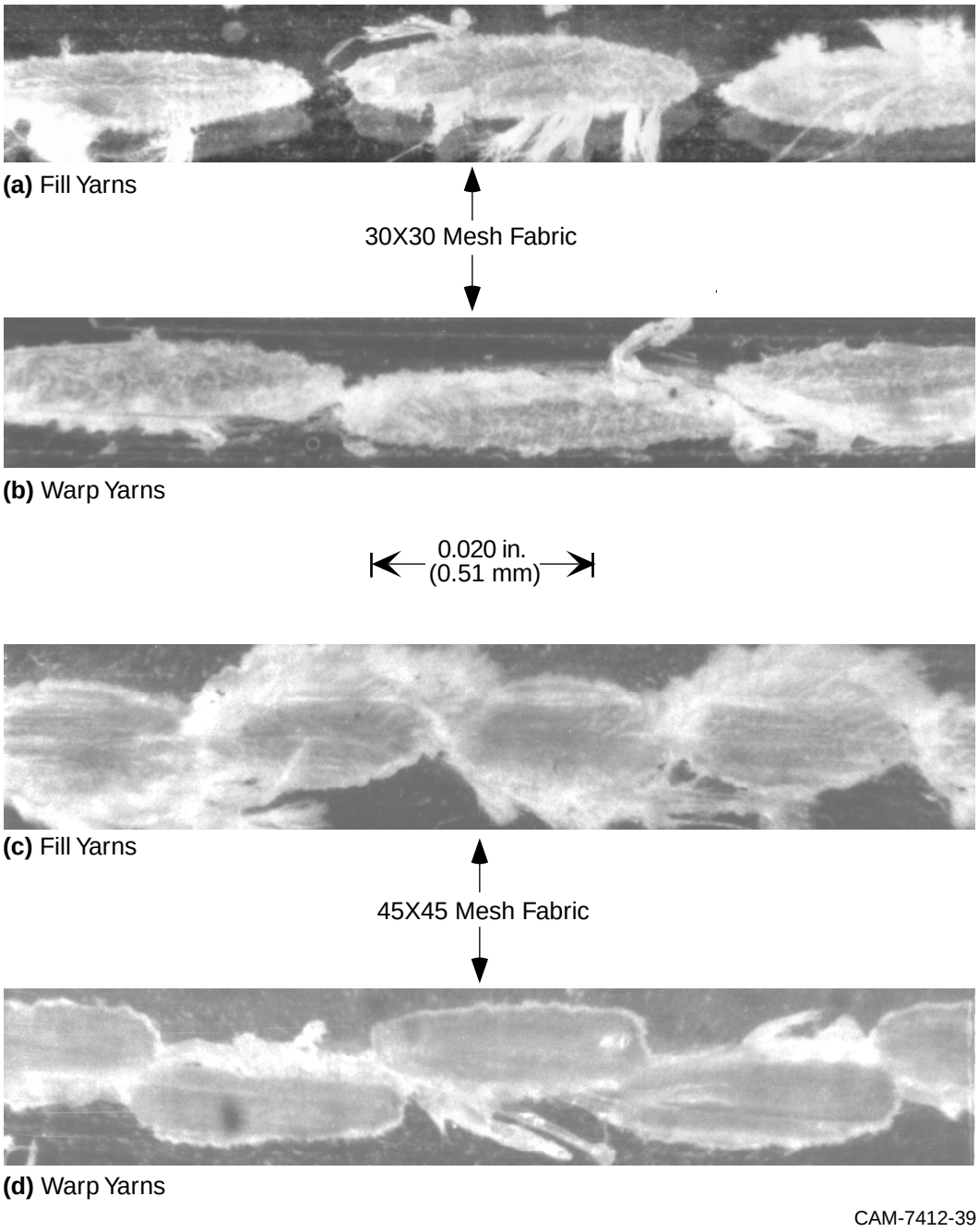

FIGURE 8. CROSS SECTIONS OF TWO ZYLON FABRICS SHOWING SHAPE AND POSITION OF FILL AND WARP YARNS

materials. As expected, the 30 x 30 mesh yarns are thinner and more widely separated with an aspect ratio of ≈5, and the 45 x 45 mesh yarns are thicker and more bunched together with an aspect ratio of ≈2.5 to 3. Adjacent fill yarns from both meshes have only a negligible offset with

respect to each other, and warp yarns have a larger relative offset, particularly for the 45 x 45 mesh where the offset is a significant fraction (perhaps 70%) of the total yarn thickness.

Some yarns from the various fabrics were carefully removed, and their length when straightened was compared to their effective length within the fabric. This degree of crimping is an important parameter for explicit yarn modeling; it affects how much the fabric can deform without stretching the yarns along their axis. Table 4 shows this parameter for all four Zylon weaves. The fill yarn exhibits only a 0.6% increase in length, and the warp yarn exhibits a length increase that varies from 0.6% in the 30 x 30 mesh to 10.5% in the 45 x 45 mesh. Thus, the 30 x 30 mesh fabric is nearly symmetric, or isotropic, along the fill and warp directions. The fabric with higher-density meshes are more asymmetric between the fill and warp directions.

The data on fabric crimping, as well as the data on yarn size, shape, and relative locations, was used to set up the computational model.

TABLE 4. PERCENT INCREASE IN ZYLON YARN LENGTH WHEN REMOVED FROM FABRIC AND STRAIGHTENED

Mesh Yarn Type	30 x 30	35 x 35	40 x 40	45 x 45
Fill Yarns	0.6%	0.6%	0.6%	0.6%
Warp Yarns	0.6%	2.0%	5.2%	10.5%

TENSILE TESTS ON ZYLON YARNS. To provide constitutive data for the modeling effort, in particular to determine the flow curve and failure conditions, tensile tests were performed over a range of strain rates on individual Zylon yarns removed from the woven fabric. The tests were performed at SRI's servo-hydraulic testing facility, using the 20,000-lb MTS[3] testing machine. The load and stroke histories were recorded during the test and used along with the specimen cross section and gage length to calculate the engineering stress and strain histories.

Figure 9 shows a schematic diagram of the test setup. A pair of modified clevis fixtures were used to grip the yarns securely. The yarn is positioned in a narrow groove cut into the 3/4-in.-diameter smooth rod, a thin compression plate fits snugly into the groove, and the yarn is tightly gripped by bolting a clamping plate against the compression plate. The plate and rod are rounded slightly where they contact the yarn to minimize stress concentrations. For some of the tests, the yarn is held in one straight segment between the two grips. For other tests, the yarn is looped around one or both of the smooth rods so that multiple lengths of the same yarn are stretched simultaneously (improving the signal-to-noise ratio in the load cell measurements).

[3] MTS Systems Corporation, Eden Prairie, MN.

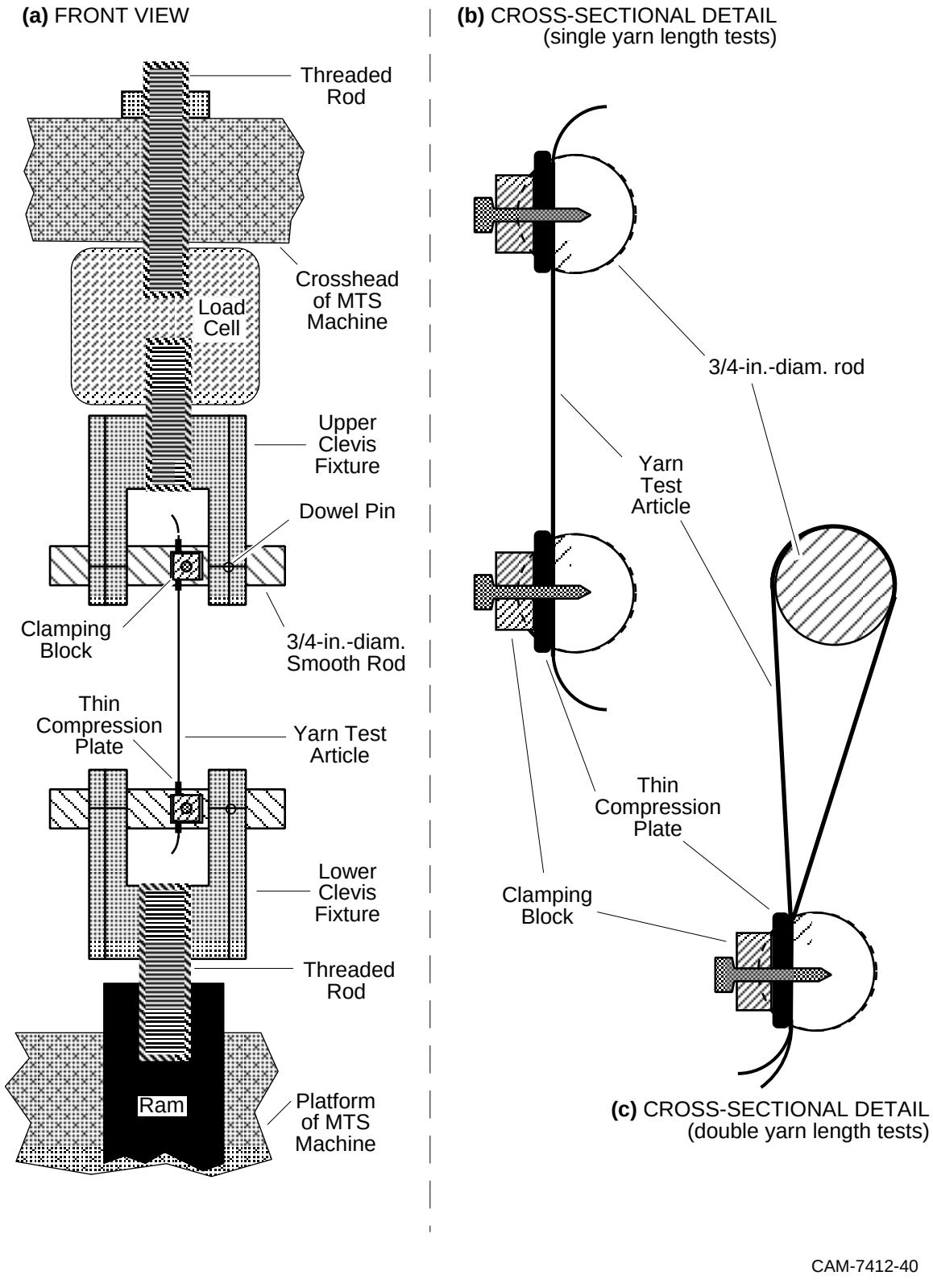

FIGURE 9. EXPERIMENTAL SETUP FOR MTS YARN PULL TESTS

Because the yarn is made up of hundreds of filaments with lots of empty space around them, the cross-sectional area of the yarn cannot simply be measured. The area, however, can be calculated by dividing the linear density (or denier) of the yarn by the bulk density of the material (1.54 g/cm^3 for PBO-AS). According to the manufacturer, all of the Zylon fabrics contained yarns that were 500 denier, but it was necessary to check this nominal value. After carefully removing the yarns from the fabric in a manner that minimized snagging of constituent filaments, the yarn's length and weight were measured. A significant variation was found (from -10% to +16%) in the actual denier value as compared with the nominal value; values from 450 to 570 denier were measured in yarn from various Zylon fabrics.[4]

The initial tensile tests were performed with fill fibers that were removed from a 30 x 30 mesh Zylon fabric. Table 5 shows a matrix of these tests. The strain rates range over a factor of 200, from 1.6 x 10^{-3} s^{-1} to 3.2 x 10^{-1} s^{-1}. Figure 10 shows the engineering stress-strain curves for four of these tests. The modulus and the tensile strength exhibit a significant strain-rate dependence, and the strain to failure appears to have a negligible strain-rate dependence. As the strain rate increases, the moduli vary from 164 to 180 GPa (24 to 26 Msi) and the tensile strengths vary from 2.75 to 3.45 GPa (400 to 500 ksi). The strain to failure remains relatively constant at ≈2.45%.

TABLE 5. TENSILE TEST MATRIX: FILL YARNS FROM ZYLON 30 x 30 MESH FABRIC

Test No.	Measured Yarn Parameters						Yarn Lengths Pulled[c]	Gage Length (in.)	Stroke Rate (in./s)	Strain Rate (1/s)
	Length (in.)	Mass (mg)	Linear Density[a]		Cross Section Area[b]					
			(mg/cm)	(denier)	(cm^2)	(in^2)				
1	49.25	71	0.565	509	3.67e-4	5.69e-5	1	34.25	0.075	2.19e-3
2	49.13	79	0.631	568	4.10e-4	6.35e-5	1	28.68	0.075	2.62e-3
3	49.56	79	0.628	566	4.08e-4	6.32e-5	6	47.57	0.013	1.58e-3
4	49.19	62	0.498	448	3.23e-4	5.01e-5	6	47.39	0.013	1.58e-3
5	49.19	70	0.557	501	3.62e-4	5.61e-5	2	46.90	0.038	1.60e-3
6	49.19	70	0.563	507	3.66e-4	5.67e-5	2	47.11	0.038	1.60e-2
7	49.19	71	0.565	509	3.67e-4	5.69e-5	2	47.11	0.375	1.60e-2
8	49.25	63	0.503	453	3.27e-4	5.06e-5	2	46.86	7.5	3.20e-1
9	49.19	63	0.500	450	3.25e-4	5.04e-5	2	46.86	3.75	1.60e-1

[a] Denier is defined as grams per 9 kilometers.

[b] Equals the volume density (which is 1.54 g/cm^3 for PBO-AS) divided by the linear density.

[c] See figure 9 for explanation.

[4] From one sheet of 30 x 30 mesh fabric, eight consecutive fill yarns were removed and a very consistent pattern of alternating denier values was found. The odd-numbered yarns were all 505 ± 4 denier, and the even-numbered yarns were all 457 ± 4 denier. Two spools of yarn were apparently used to weave the fill yarns of this fabric; there is little denier variation within a single spool, but different spools had significantly different denier values.

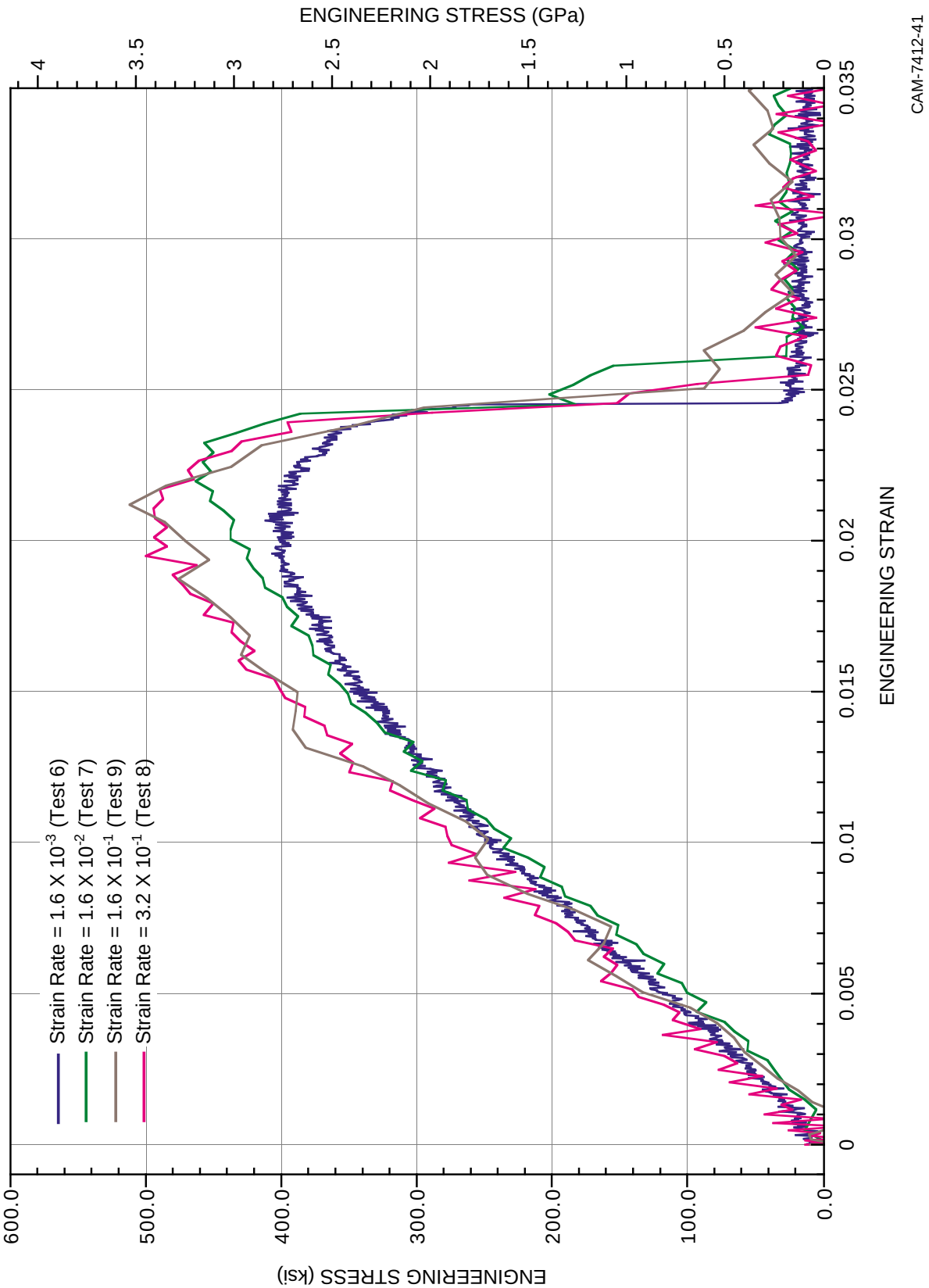

FIGURE 10. TENSILE TEST RESULTS FOR FILL YARNS REMOVED FROM ZYLON 30 x 30 MESH FABRIC

The manufacturer's values for the PBO-AS fiber are as follows: modulus of 180 GPa (26 Msi), tensile strength of 5.8 GPa (840 ksi), and strain to failure of 3.5%. So the measured modulus for the yarn is similar to that of the fiber, but the measured tensile strength for the yarn is roughly half of that for the fiber, and the strain to failure is about 70%. The manufacturer has suggested that the weaving process itself may degrade the strength of the yarns, so it is planned to test unwoven yarn in the next year.

A more likely explanation for a large part of this difference is that the filaments do not all fail at the same time in a yarn tensile test. All of the hundreds of filaments that make up a single yarn cannot be gripped with precisely the same amount of tension. Some of the filaments in a yarn carry a higher load than others and fail sooner (at a lower stroke), leaving a smaller cross-sectional area to withstand the remaining load. The same phenomenon would be expected to occur in a fragment impact scenario, so the values obtained for the yarn in the tensile tests are the ones used in the computational model.

The energy that it takes to fail the yarns can be determined by calculating the area under the load-deflection curves. For the curves shown in figure 10, the energy to break the yarn is about 1.9 J (1.4 ft-lbs). As a comparison, for gas gun impact Test 20, in which the 25-g FS penetrated a single ply of the Zylon 30 x 30 fabric and broke 39 yarns in the process, the energy absorbed was 30.5 J (22.5 ft-lbs), which is only 0.78 J (0.58 ft-lbs) per broken yarn. But the fact that the gage length in the tensile tests (≈47 in.) is much greater than the grip separation in the gas gun tests (7.5 in.) must be accounted for. Because the energy absorbed in breaking a yarn is proportional to the yarn length, a tensile test using a gage length of 7.5 in. would require an energy of only 0.3 J (0.22 ft-lbs) to break the yarn. So why is this energy significantly less than the energy per broken yarn in the gas gun tests?

Two reasons are offered. First, and most significantly, in the gas gun tests the impactor is, in addition to breaking the 39 yarns directly in its impact path, using energy for inelastic deformation of the entire fabric target (e.g., mesh distortion, frictional sliding of yarns, etc.). Second, there may be a strain-rate effect. The strain rate in the gas gun tests can be determined very roughly. The FS was observed to penetrate the fabric approximately 1/3 ms after impact at a fabric deflection (at the impact region) of slightly over 1 in. This yields a yarn strain rate of roughly 75/s which is significantly larger than the highest strain rate tested in the tensile tests of 0.16/s. As discussed below, it is expected to increase the tensile test strain rates by nearly two orders of magnitude which should be close enough to those in the impact tests to significantly reduce uncertainties in the strain-rate dependency.

QUASI-STATIC PENETRATION (PUSH) TESTS. A quasi-static penetration test ("push test") was designed and implemented that allowed a rigidly held fragment or FS to be push into a high-strength fabric (or other) target at velocities ≤ 7.5 in/s while simultaneously recording the deflection and the load. If desired, high-resolution video pictures of the target deformation and failure can also be taken. The purpose of this type of test is to provide a better understanding of

the mechanisms and the evolution of deformation and failure during a fragment penetration of a target barrier and then use this information to aid in model development, calibration, and verification. A variety of fabric materials, configurations, and boundary conditions can be investigated.

The push test is similar to a gas gun impact test in that the same impactor is used, and the targets can have the same boundary conditions in both types of tests. Advantages of the push test (as compared with the gas gun test) are listed below:

- There is more control over the impactor (or more precisely the pusher). The pitch, yaw, and roll can be precisely predetermined, and the stroke can also be stopped at any point and the damage in the target can be closely examined.

- The diagnostics are better. The target surfaces can be observed from various angles with much greater resolution, and the deformation and failure of individual yarns can be recorded which relates the breaking of a particular yarn to a specific sharp drop in the load-deflection curve.

- The push test can be used as a model verification test because a record now exists of the load and deflection histories (and if a video is used, there is a record of fabric shapes and individual yarn deflections and failures), not just the energy absorbed and the posttest sample.

- Cost and turnaround time are significantly less, so more tests can be performed, varying the target design, for example, until a desired target parameter is optimized. This reduces the number of gas gun tests that need to be performed. (However, the maximum push velocity is several orders of magnitude less than the impact velocity in the gas gun test. Therefore, gas gun tests must still be performed to demonstrate fragment barrier effectiveness at actual impact velocities occurring in engine fragment scenarios to confirm the deformation and failure processes observed at lower strain rates in the push tests).

Experimental Setup. The push test is performed on the same MTS System Corporation servo-hydraulic testing machine used in the yarn tensile tests. Figure 11 shows the experimental configuration. The target is mounted and clamped horizontally on the same mounting frame and support structure used in the gas gun impact tests. This structure is attached, through a load cell, to the MTS machine's crosshead. The FS (or other pusher fragment) is rigidly attached to the top of the ram. During the test, the ram strokes upward forcing the rod into and through the target.

Figure 12 shows the photographic setup that can be used with the push tests. A front-surface mirror is positioned inside the support structure at approximately 45° to the target surface. The back surface of the target is illuminated (specifically the region around the pusher contact zone) by a strong light reflecting from the mirror. A video camera is positioned to look

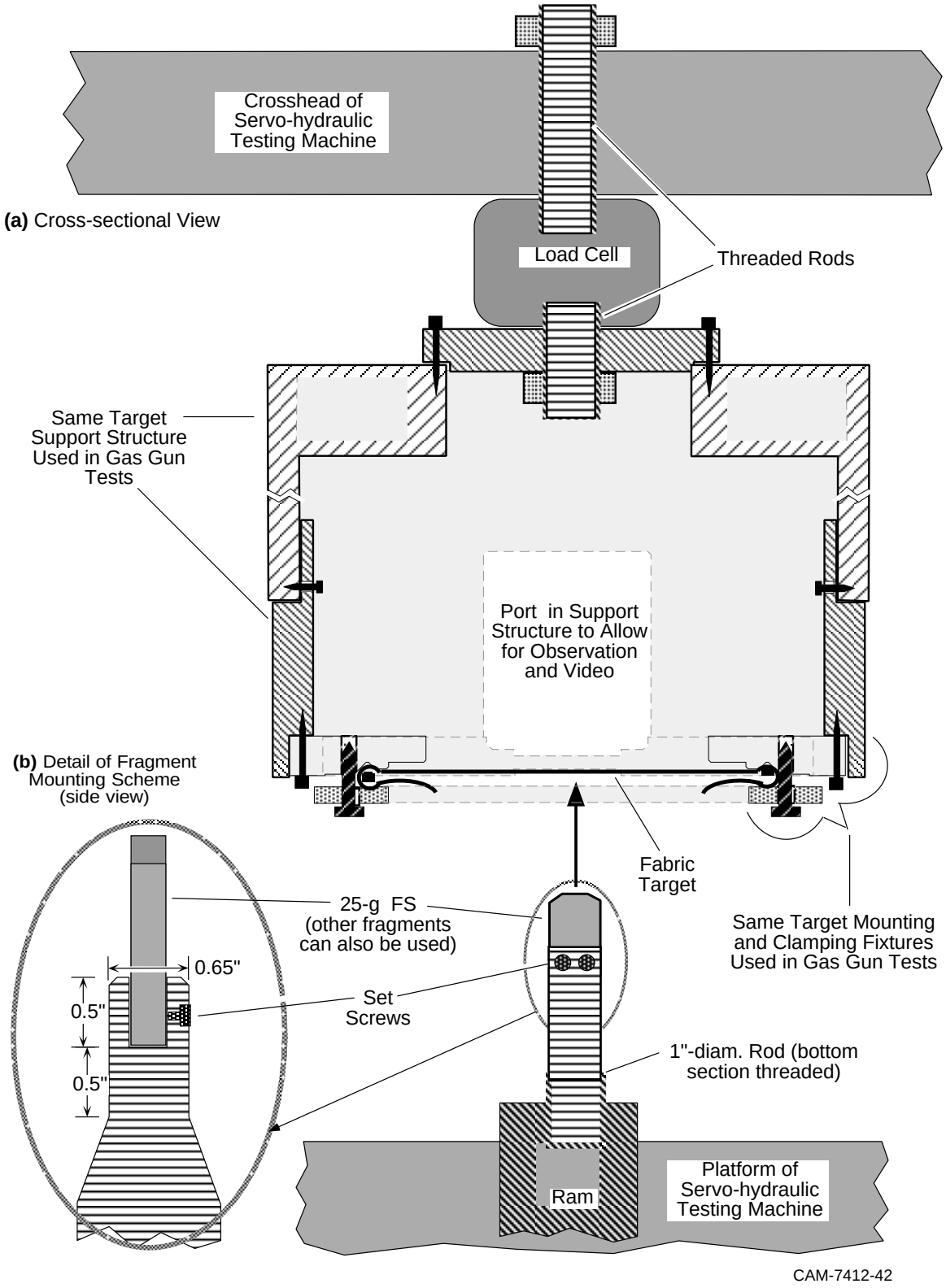

FIGURE 11. EXPERIMENTAL ARRANGEMENT FOR FRAGMENT PUSH TESTS

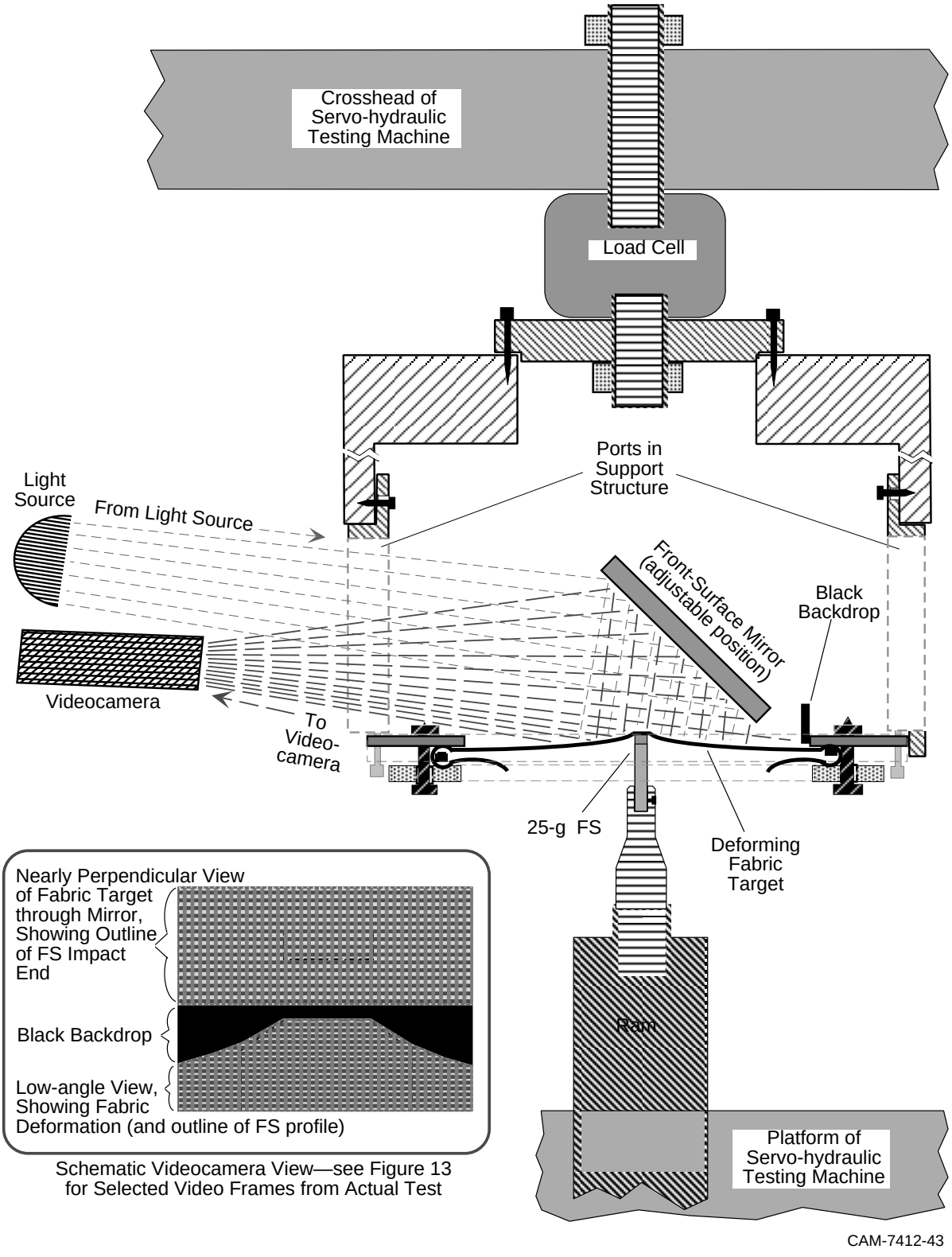

FIGURE 12. VIDEO CAMERA AND LIGHTING ARRANGEMENT USED IN CONJUNCTION WITH FRAGMENT PUSH TESTS

simultaneously at two regions (see the inset in figure 12): directly at the back surface of the target (at a very low angle) to show the shape of the deforming fabric and at the same region through the mirror (at an angle of ≈90°) to observe yarn failure. The camera can be zoomed in to allow resolution of individual yarns.

Preliminary Test Results. An initial series of six push tests were performed using single-ply sheets of Zylon 35 x 35 mesh fabric. Table 6 shows a matrix of parameters and some results for this series. The clamping scheme and the shape of the fabric sheets are identical to that used in the impact tests (see figure 2(a)). In all of the tests, the 25-g FS was pushed at 0° pitch and 0° yaw into the fabric, which was tightly gripped parallel to both the fill and warp yarns directions.

TABLE 6. PUSH TEST MATRIX FOR 25-g FRAGMENT SIMULATOR INTO SINGLE-PLY ZYLON 35 x 35 WEAVE TIGHTLY GRIPPED ON FOUR SIDES

Test No.	Video	FS Orien-tation[a]	Stroke Rate[b] (in./s)	First Yarn Break		Failure Stroke[c] (in.)	Maximum		Yarns Broken (Warp+fill) =	Work[d] Done (J)
				Stroke (in.)	Load (lb)		Load (lb)	Modulus (lb/in.)		
P-1	—	0°	0.075	0.873	863	0.890	894	3640	7 + 30 = 37	19
P-2	—	0°	0.075	0.764	838	0.803	916	3389	8 + 30 = 38	22
P-3	—	0°	7.5	0.802	909	0.828	955	3386	8 + 32 = 40	22
P-4	—	0°	0.075	0.796	895	—	897	4087	8 + 0 = 8	14
P-5	Yes	0°	0.0075	0.792	792	0.832	853	3040	8 + 31 = 39	20
P-6	Yes	90°	0.0075	0.723	695	0.768	816	2980	26 + 8 = 34	17

[a] For 0° orientation, long dimension (1 in.) of FS cross section is parallel to warp yarns; for 90° orientation, long dimension is parallel to fill yarns.

[b] Tests involve constant stroke rate to complete penetration except test P-4 which involved cyclical loading and test interruption prior to complete penetration.

[c] Stroke at complete penetration (where load drops to zero).

[d] Equals the area under the load-deflection curve.

Figure 13 shows portions of selected video camera frames taken during Test P-6. Individual yarns are clearly visible. The overall deformation profile can be seen as can the individual yarns that break at late stages in the deformation, but before complete fabric perforation. These individual yarn failures can be precisely correlated to the load-deflection curve (shown in figure 14). The inset shows three sharp drops in the load which occur as a result of one or more individual yarn failures. The first of these drops corresponds to the first yarn failure depicted in the consecutive video frames (c) and (d) in figure 13.

Based on (1) the video pictures, (2) the popping sound that accompanies each yarn break, and (3) the drops in the load histories, roughly four to eight yarns appear to break noticeably in advance of complete fabric penetration. For tests P1 through P-5, in which the longer dimension of the FS's cross section was perpendicular to the fill yarns, all of the early yarn breaks were fill yarns located at the corners of the impact end of the FS. For Test P-6, whose FS orientation was 90° to that in the other tests, the first yarn to break was a fill yarn located at the FS corner but subsequent broken yarns were warp yarns.

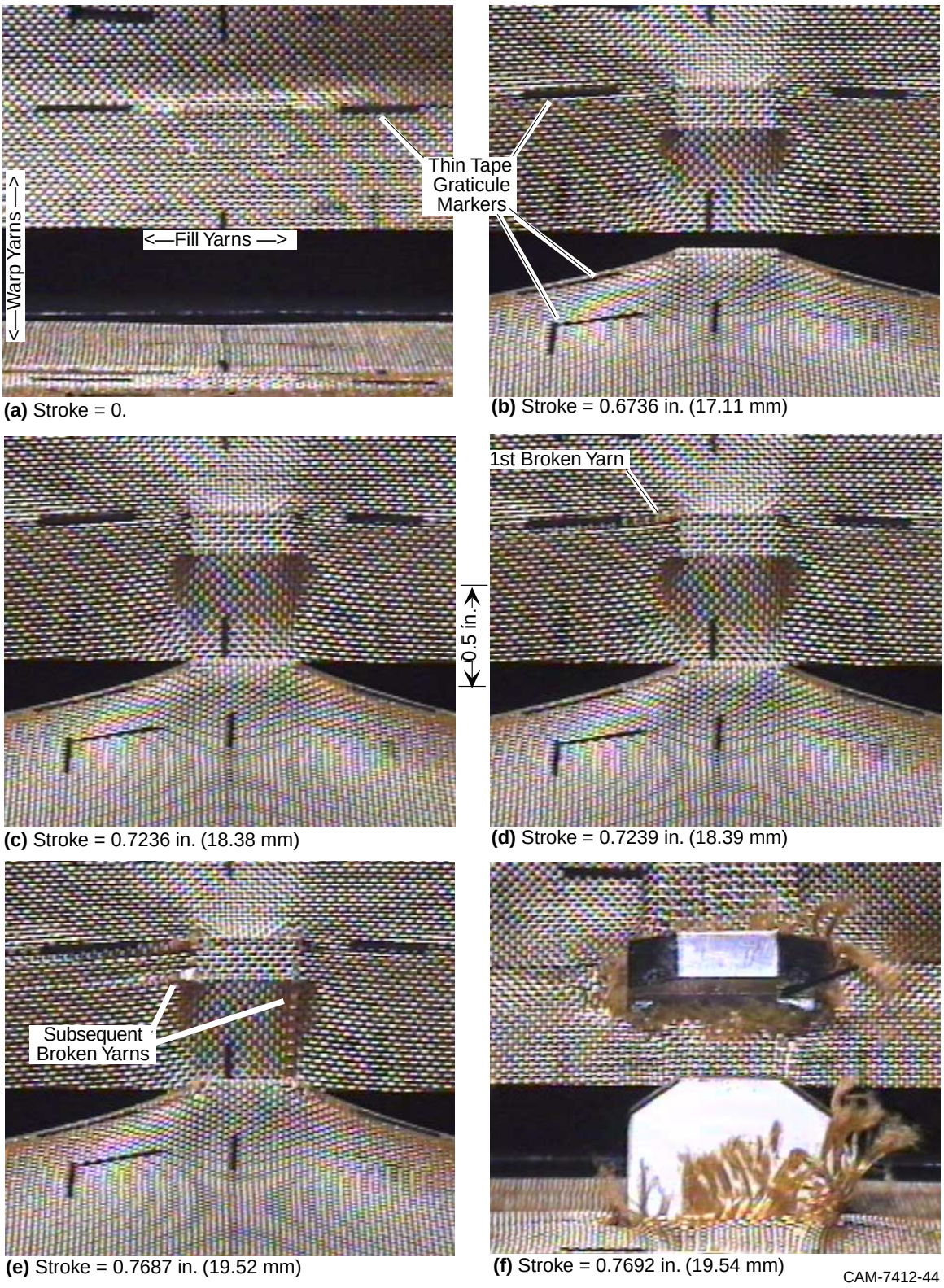

FIGURE 13. SELECTED VIDEO CAMERA FRAMES OF ZYLON FABRIC DEFORMATION AND FAILURE IN PUSH TEST P-6
(See figure 12 inset or explanation of video images.)

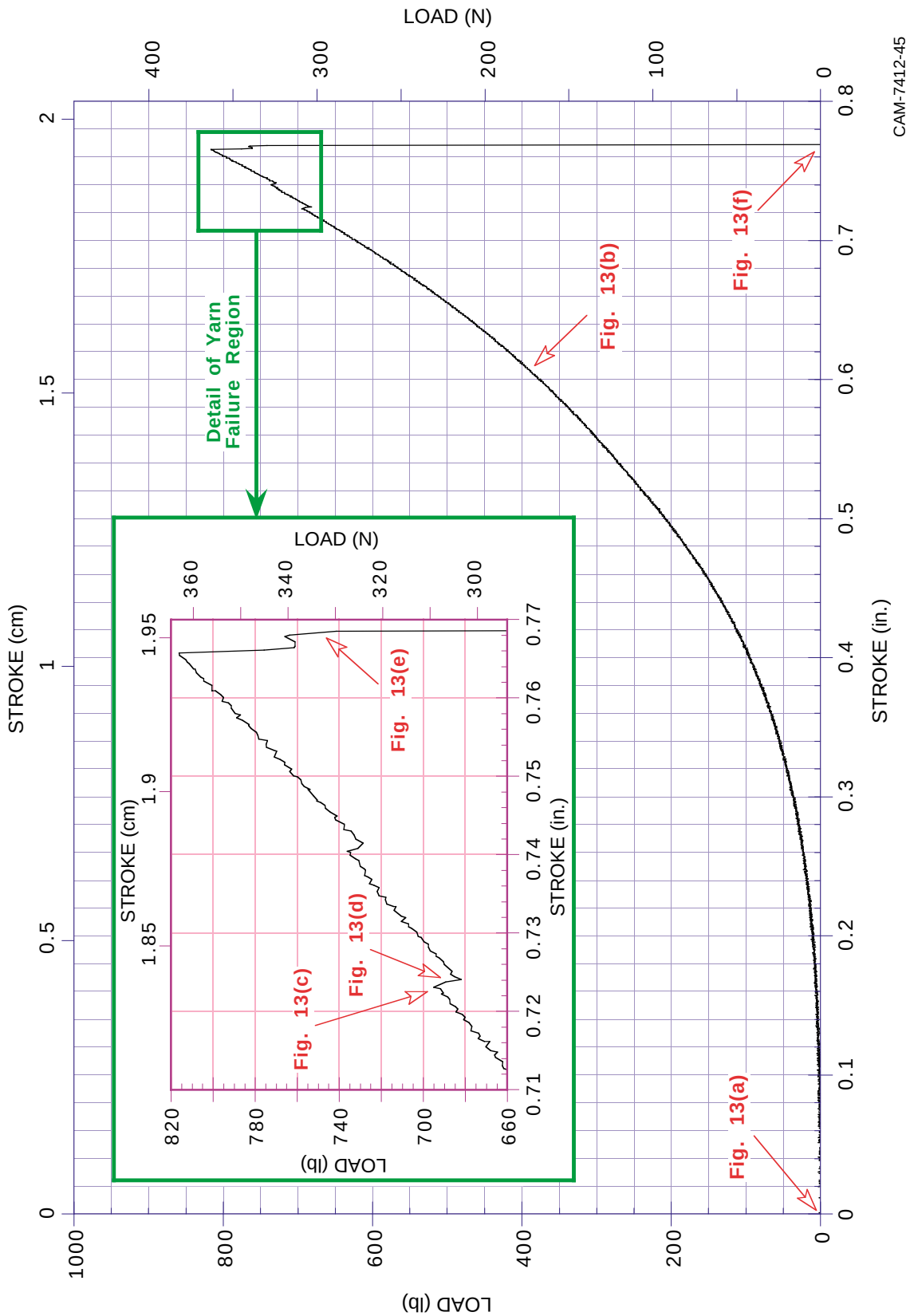

FIGURE 14. LOAD-DEFLECTION CURVE FROM PUSH TEST 6: 25-g FRAGMENT SIMULATOR INTO SINGLE-PLY ZYLON 35 x 35 MESH FABRIC AT STROKE RATE OF 0.0075 in./s (Red arrows point to load and stroke values at the time of the video images shown in figure 13.)

Analysis. Figure 15 shows the load-deflection curves for all of the tests involving constant stroke rate to failure. These tests cover a range in stroke rates of three orders of magnitude. To investigate any strain rate trends, four parameters (load at first yarn break, peak load, stroke at first yarn break, and stroke at fabric penetration) were plotted, in figure 16, as a function of the stroke rate. Both the load at first yarn break and the peak load as a function of stroke rate increase monotonically, but there is no clear stroke-rate dependence on either of the stroke parameters. This observation is in agreement with the results of the yarn pull tests where a clear strain-rate dependence for tensile strength was evident but not for strain to failure.

Furthermore, the stroke values are very likely dependent upon the pretensioning of the fabric during clamping. Although attempts were made to apply the same traction to the fabric during clamping, it is known that the same level of pretension cannot always be attained. A lower-pretensioned fabric should reach the same values for load but would reach them at larger strokes. The fabric in Test P-1, for example, was not stretched as tautly before clamping (the test was performed before a pretensioning apparatus was constructed), and it has significantly higher stroke values at the same levels of load as the other tests. The stroke values could be shifted by a constant value (without any resultant change in the load, moduli, or work done), and the curves would lie in closer proximity to each other.

In conclusion, the push test cannot take the place of actual impact tests because of the rate dependency observed in the failure strength. However, the push test appears to be a very good method of characterizing the mechanisms and evolution of high-strength fabric failure and is therefore a very useful tool to help develop, calibrate, and verify models for fragment impact and penetration. More push tests will be performed on a wide variety of materials and geometries in the near future.

COMPUTATIONAL MODEL DEVELOPMENT.

During this first year of Phase II, development of models to perform finite element simulations and analyses of fragment impact experiments were started. The experiments are highly dynamic events, three-dimensional in nature, and include strong nonlinear effects such as impact, penetration, and failure of materials. Thus, the requisite models for analysis are highly complicated. The analysis is used to guide and understand the impact experiments, and the experiment results are used to guide development of the models. The overall understanding of the impact mechanics can then be used to design impact resistant barriers. Good models will allow parameter studies to help optimize barrier designs and to investigate new materials.

The analyses to date have focused on two types of materials: aluminum fuselage skin (2024-T3) and woven fabrics of high-strength polymers, particularly Zylon. To perform the analyses either of the finite element codes DYNA3D or LS-DYNA3D was used. DYNA3D is an explicit, three-dimensional, nonlinear, finite element code for analyzing the dynamic response of structures. Modifications were made to the SRI version of DYNA3D to include a library of advanced

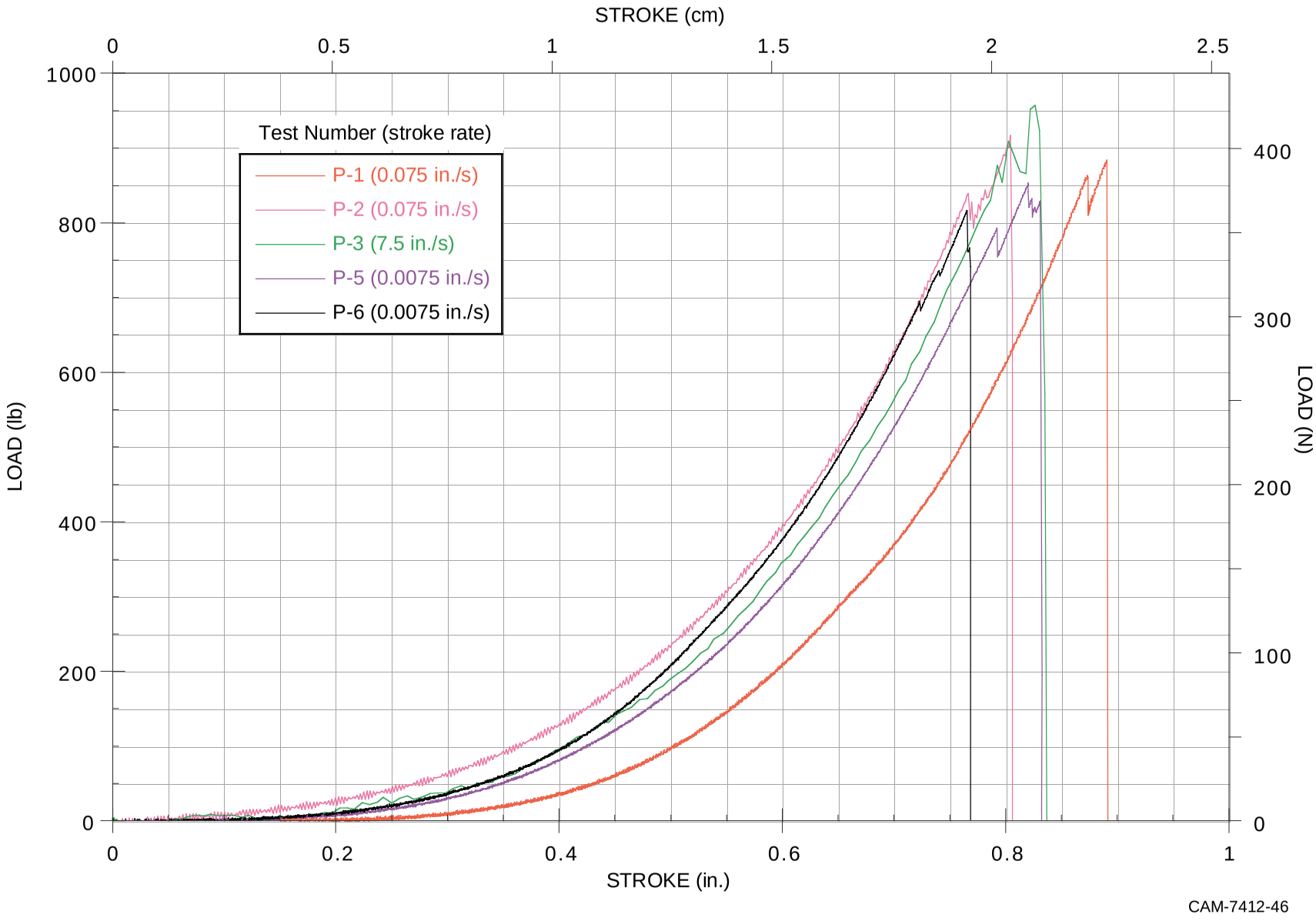

FIGURE 15. LOAD-DEFLECTION CURVES FROM NONCYCLICAL PUSH TESTS P-1 THROUGH P-6: 25-g FRAGMEMT SIMULATOR INTO SINGLE-PLY ZYLON 35 x 35 MESH FABRIC

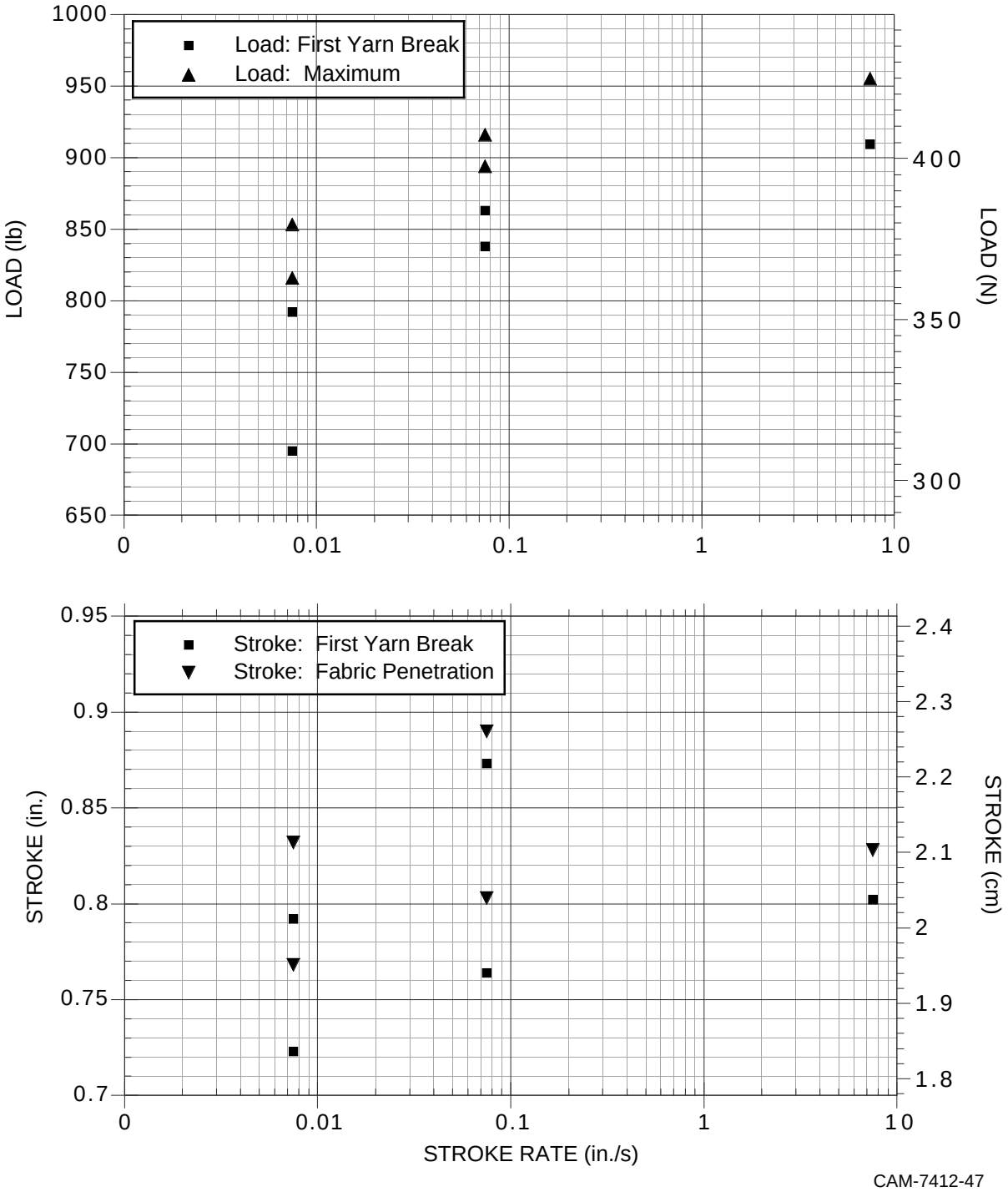

FIGURE 16. LOAD AND STROKE MEASUREMENTS AS A FUNCTION OF STROKE RATE FOR PUSH TESTS P-1 THROUGH P-6 (Tests involve 25-g FS into single-ply Zylon 35 x 35 mesh fabric.)

material constitutive/damage models and advanced fracture algorithms. LS-DYNA3D, a derivative of DYNA3D, developed by J. Hallquist at Livermore Software, has a wide range of material models and contact algorithms. The codes were run on a local network of SGI computer workstations. Both codes are in the public domain.

The computational ability to predict the response of aluminum fuselage skin was described and demonstrated in a previous report.[5] Described here is our approach, progress, and plans to develop a similar computational ability for woven fabric.

SIMULATION OF WOVEN FABRIC. SRI International is developing a finite element model for woven fabrics. The model starts with explicit modeling of the individual yarns that make up the fabric. This will allow analysis of fiber-to-fiber interactions during impact and help in understanding the origins of the attractive ballistic behavior of polymer fabrics.

Figure 17 shows the finite element model configuration for a woven fabric. Fill (figure 17(a)) and warp (figure 17(b)) yarns are modeled individually and then combined to form a fabric mesh (figure 17(c)). The finite element model configurations for shapes and geometry of the yarns were taken from high-resolution photographs of actual fabrics used in the testing. As shown in the figure, the weave is not symmetric.

MODELING APPROACH. The material model and properties used for the yarns were based on individual yarn pull tests. Mechanical properties for the yarn are listed in table 7. An elastic-plastic model was used for the yarn with a modulus of 164 GPa (24 x 10^6 psi) and a strength of 3.2 GPa (465 ksi). The strain to failure was measured at about 2.5%.

Initially a wavy yarn was modeled and pulled to failure; the response is shown in figure 18(a). The initial wavy yarn straightens out, and when the failure stress is reached, the failed element is eroded and failed sections are removed from the calculation. Figure 18 shows the calculated and measured stress-strain curves for the yarn. The simulation shows very good agreement with the test results.

EXAMPLE SIMULATIONS. To see if the model would produce the desired type of results for fragment impact against woven fabrics, several simple simulations were performed using a square patch of fabric fixed at boundaries, only a limited number of yarns, and a very small fragment. Two simulations were performed; one at an impact velocity of 20 m/s and another at 80 m/s. At 20 m/s there was no damage to the fabric and the impactor rebounded from the fabric with essentially an elastic response. At 80 m/s, as shown in figure 19, the impactor penetrated the weave and continued on through the fabric. These results demonstrated the basic efficacy of the model and show that the model is suitable for development.

[5]D. A. Shockey, J. H. Giovanola, J. W. Simons, D. C. Erlich, R. W. Klopp, and S. R. Skaggs, "Advanced Armor Technology Application Potential for Engine Fragment Barriers for Commercial Aircraft," SRI International Final Report to Federal Aviation Administration (DOT/FAA/AR-97/53), Atlantic City International Airport, NJ (September 1997).

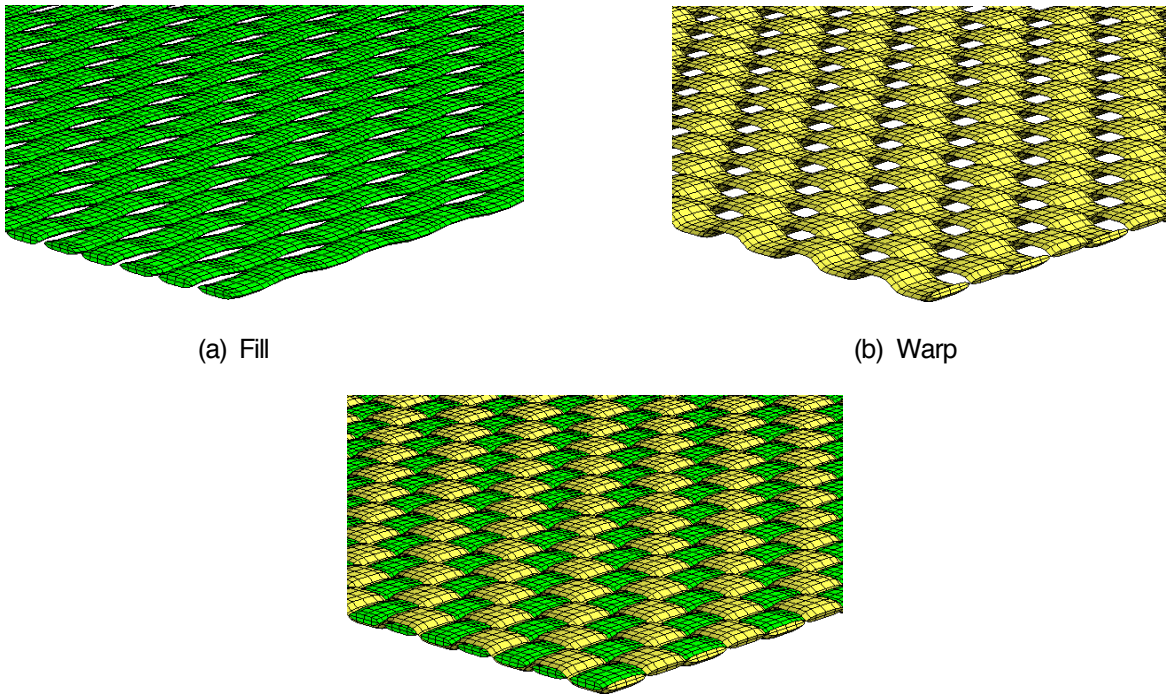

FIGURE 17. FINITE ELEMENT CONFIGURATION FOR WOVEN FABRICS

TABLE 7. ZYLON YARN PROPERTIES

Weight	500 denier
Modulus	164 GPa (24 x 10^6 psi)
Strength	3.2 GPa (465 ksi)
Strain to failure	2.5%
Geometry	30-45 threads per inch

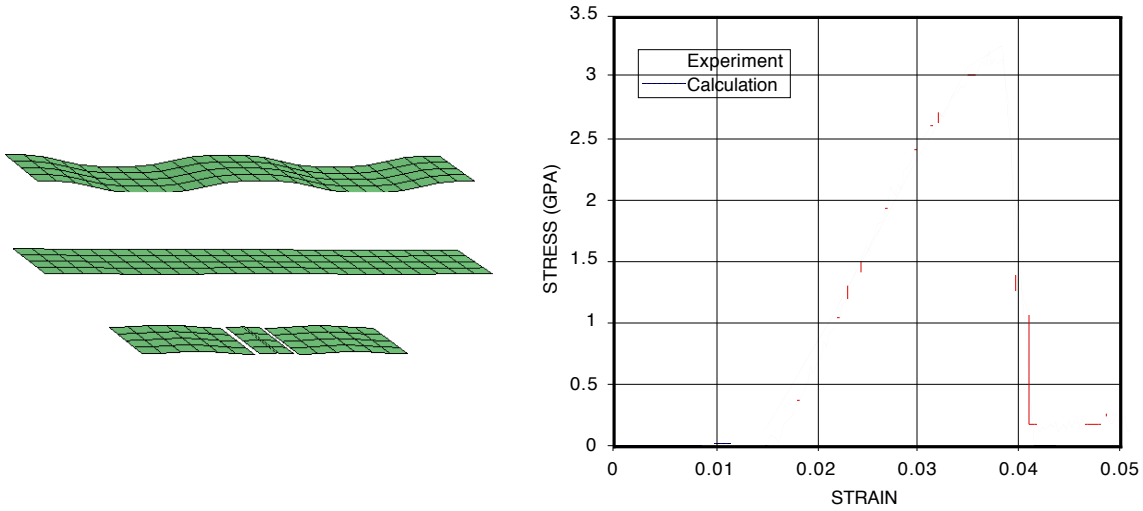

(a) Yarn response (b) Yarn stress-strain curve

FIGURE 18. RESPONSE OF A ZYLON YARN

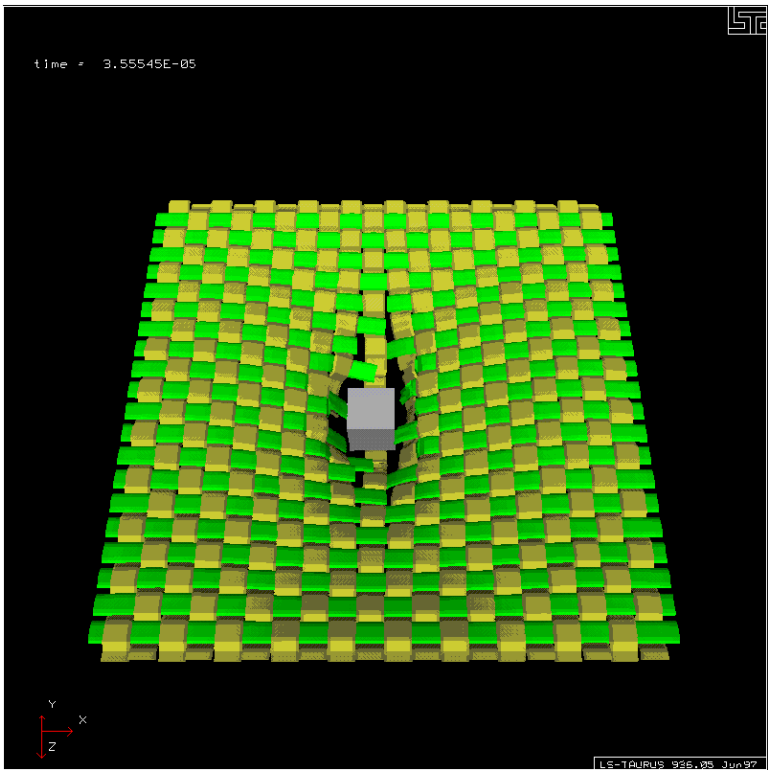

FIGURE 19. EXAMPLE SIMULATION OF A SMALL FRAGMENT PENETRATING THE FABRIC AT 80 m/s

MODEL DEVELOPMENT. SRI is extending its fabric model to simulate the tests performed on Zylon fabric. Many more threads and a larger impactor are being modeled. Figure 20 shows some example configurations with thread densities of 5 and 10 threads per inch. It is assumed that at some thread density (less than the 30/inch in the experiment) the model will act like a fabric and can be studied to learn about the response mechanisms. The increase in number of elements and the large increase in impactor energy has introduced some numerical instabilities in these calculations. In particular, the contact routines have numerical difficulty in preventing element interpenetration because the yarn-to-yarn interaction is relatively compliant compared with the stiff impactor. Options are being investigated for defining the contact algorithms and the slideline penalties. Currently, each calculation entails on the order of 100,000 elements and takes several days to complete on a workstation.

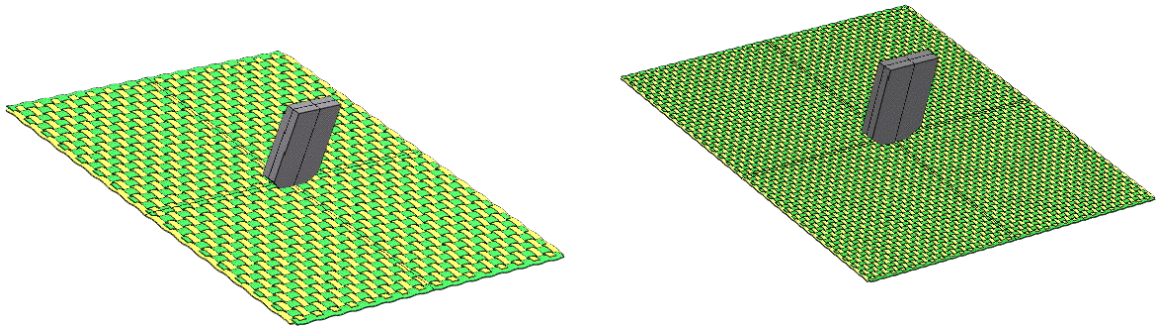

FIGURE 20. EXAMPLE CONFIGURATIONS FOR SIMULATING FABRIC TESTS

PLANS

SRI International is planning (or are in the process of performing) experiments of the following types: yarn tensile tests, push tests, impact tests at SRI, and impact tests at China Lake. Each of these tests is describe below.

YARN TENSILE TESTS.

To help develop the computational models, SRI plans to conduct additional tensile tests on individual Zylon yarns (and perhaps yarns from other high-strength fiber materials). Already tested are fill yarns from the 30 x 30 mesh fabric, a yarn that is only slightly crimped during the weaving process (see figure 8 and table 4) and plans are to test more highly crimped yarns (e.g., warp yarns from 40 x 40 or 45 x 45 mesh fabric) to determine the effect of crimping on the tensile strength and strain-to-failure. Results from these tests will tell us if we can use the same constitutive properties for the warp and fill yarns in the computer models or if different constitutive properties for the two types of yarn are needed. SRI also plans to perform a few tests on unwoven yarn to determine the effect of weaving on yarn strength (if weaving drastically

decreases yarn strength, it might be necessary to consider using unwoven fabrics as a barrier material).

In addition, with some minor modifications to the test setup and procedure, SRI expects to perform yarn tensile tests at strain rates as high as ≈10/s (as compared to the current maximum of 0.16/s). These tests will yield constitutive properties at strain rates much closer to those occurring in actual impact tests (estimated at ≈75/s) and will reduce the extrapolation needed to calibrate the computational models.

PUSH TESTS.

To continue the examination of the mechanisms and evolution of high-strength fabric fragment barrier deformation and penetration, SRI plans to conduct a wide variety of push tests during the coming year. Experimental parameters are planned to include

- Fragment size, orientation, and shape.[6] SRI has obtained, from Naval Air Warfare Center (NAWC)-China Lake, actual compressor/turbine and fan blades of three different sizes—they are thinner and sharper-edged than the FS and will allow studying the effects of fragment sharpness.

- Fabric material and type (e.g., weave, layup, or felt), number of plies, yarn orientation, and boundary conditions (e.g., gripped on two sides or four sides).

- Placement of high-strength felt layers in front of the fabric (In particular, if it turns out that fabric barrier failure is strongly affected by fragment sharpness, then does the felt effectively blunt sharp-edged fragments?).

The plan is to also continue investigating practical alternatives for gripping high-strength fabric fragment barriers, alternatives that exploit the high fiber strength. In particular, different methods of attaching the fabric to an IWP that would enhance energy absorption will be tested.

IMPACT TESTS AT SRI.

Using the results of the push tests to focus the gas gun test matrix, SRI plans to perform additional impact tests using its 4-in.-bore gas gun to launch either FSs or actual compressor, turbine, and fan blade fragments at realistic fragment velocities. The same parameters as listed above for the push tests will be varied with the principal purpose being to determine the effect upon the specific energy absorption (SEA). One series will involve full-penetration impact tests

[6] (At a 45° roll angle with respect to the yarn orientation, for example, the impact end of a fragment will intersect and need to break ≈50% more yarns than at 0° to achieve penetration. At a 45° pitch or yaw angle, a fragment presents more of a cross-sectional area to a fabric than at a 0° pitch or yaw but may deflect some of these yarns sideways, rather than break all of them, to achieve penetration. Also, the target (particularly a multiple-ply target) may rotate the fragment during penetration, decreasing the hole size and reducing the number of broken yarns on successive target plies.)

with rigidly held, multiple-ply Zylon fabric targets to determine the effect of larger numbers of plies on the SEA (the maximum number of plies for which SRI has full-penetration data is four).

IMPACT TESTS AT CHINA LAKE.

Working with Joseph Manchor and Chuck Frankenberger of NAWC, SRI International designed impact tests involving high-strength fabric targets to be performed at the new gas gun facility at China Lake as part of the FAA Engine Debris Penetration Test series. The first series of these tests, scheduled for the spring of 1998, will involve compressor/turbine blade fragments impacting a target consisting of multiple plies of a high-strength fabric (Kevlar or Zylon). The target will be made by continuous wrapping of a single ≈12-in.-wide sheet of fabric around two smooth, cylindrical rigid posts ≈15 in. apart, effectively gripping the target in one direction but not in the other. This boundary condition (tight gripping on two opposite sides, rather than on all four sides) is one that may be more readily adapted for easier insertion into (and removal from) a fuselage framework.

SRI may also try impact tests involving significantly larger fabric sheets, perhaps large enough to stretch over several unit cells of a fuselage framework, to investigate the effect of fabric size.

MODEL DEVELOPMENT.

SRI plans for the remainder of Phase II are to

1. Verify a working model for fabric by comparing simulations with the results of the fabric tests. This model will be of the type described above where individual yarns are modeled. The detailed model is the best way to understand the mechanics of fabric response. SRI is currently seeking solutions to several numerical problems.

2. Investigate the effect on ballistic performance of the details of the yarn properties and interactions (such as interlayer friction, tensile and shear strength of fibers, and strain to failure of fibers). The results of these analyses will help SRI identify which material properties are important in ballistic performance and thus will help guide the selection of existing materials or help define requirements for new materials.

3. Investigate changes in weave design to improve ballistic performance. The objective here would be to design the weave to involve as many yarns as possible. As shown above, the current weave designs are asymmetric—the fill yarns are tighter than the warp yarns. The analyses show that this feature causes the impactor to stress the fill fibers well before it stresses the warp fibers. Perhaps a more symmetric weave design would load the fibers more equitably and improve the ballistic resistance. We will systematically analyze and design parameters such as weave symmetry and weave pattern to determine geometries that provide improved ballistic performance.

4. Investigate the effects of boundary conditions on the ballistic performance. Any practical barrier design must rely on the strength of supports to develop the strength of the fibers. For implementation in an aircraft, SRI envisions using the existing structural members as a reaction frame and will perform analyses to determine how the existing frame can best be used to react the barrier loads or help design strategies to enhance the effectiveness of the supports.

5. Develop a continuum model for fabric. To perform calculations for multiple layers of fabric economically, a continuum model is needed for the woven fabric that captures the effects of the fabric details but does not model them explicitly. SRI envisions that the fabric model will be similar to existing continuum models for computing damage response in composites. SRI intends to use the results of the detailed fabric model to identify the important response and damage mechanisms and to calibrate the model for single-layer fabrics. The model should apply to multiple-fabric layers and layups of different design and orientation and would be implementable into DYNA3D as part of the design toolbox. Development of a working model for fabrics that is numerically robust under impact and penetration loads is a formidable undertaking.

6. Model multiple layers of fabric and fabric interacting with other materials (e.g., felt and honeycomb). Practical designs for fragment barriers will no doubt include multiple layers of fabric as well as other materials such as felts or honeycomb. Analyses of postulated hybrid barrier concepts will help to identify and validate practical barrier designs with customizable ballistic properties.

REFERENCES

1. Aircraft Catastrophic Failure Prevention Research Program, Program Plan, January 1994, U.S. Department of Transportation, Federal Aviation Administration, William J. Hughes Technical Center, Atlantic City International Airport, NJ.

2. D. A. Shockey, J. H. Giovanola, J. W. Simons, D. C. Erlich, R. W. Klopp, and S. R. Skaggs, "Advanced Armor Technology Application Potential for Engine Fragment Barriers for Commercial Aircraft," SRI International Final Report to Federal Aviation Administration (DOT/FAA/AR-97/53), Atlantic City International Airport, NJ (September 1997).